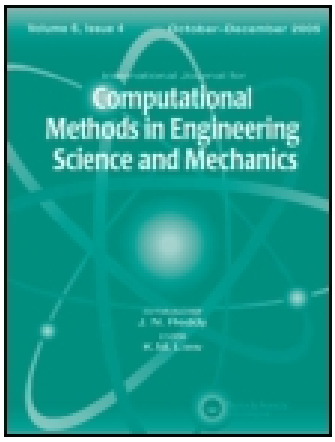

International Journal for Computational Methods in Engineering Science and Mechanics

Publication details, including instructions for authors and subscription information:
http://www.tandfonline.com/loi/ucme20

A Performance Study on Configurational Force and Spring-Analogy Based Mesh Optimization Schemes

A. Rajagopal [a], R. Gangadharan [a] & S. M. Sivakumar [a]

[a] Indian Institute of Technology, Madras, Chennai, India

Published online: 23 Feb 2007.

To cite this article: A. Rajagopal, R. Gangadharan & S. M. Sivakumar (2006) A Performance Study on Configurational Force and Spring-Analogy Based Mesh Optimization Schemes, International Journal for Computational Methods in Engineering Science and Mechanics, 7:4, 241-262, DOI: 10.1080/15502280500388169

To link to this article: http://dx.doi.org/10.1080/15502280500388169

International Journal for Computational Methods in Engineering Science and Mechanics, 7:241–262, 2006

ISSN: 1550–2287 print / 1550–2295 online
DOI: 10.1080/15502280500388169

Taylor & Francis
Taylor & Francis Group

A Performance Study on Configurational Force and Spring-Analogy Based Mesh Optimization Schemes

A. Rajagopal, R. Gangadharan, and S. M. Sivakumar
Indian Institute of Technology, Madras, Chennai, India

Assessment of *r*-adaption algorithms based on configurational force method and spring analogy approach is made. Assessment is made based on qualitative and quantitative aspects of error estimates, convergence rates and mesh quality. Appropriate modifications to node relocation procedures are proposed for enhanced performance. A simple linear projection technique is used to improve convergence characteristics of the material force node relocation algorithm. Performing mesh adaption on initial mesh results in a considerable reduction in gradients of strain energy. Assessment based on suitability of mesh adaption algorithms for structured and unstructured initial meshes has been performed. It has been observed that the configurational force method is more robust. Comparitive study indicates the superiority of the configurational force method. The proposed enhancement to the mesh adaption is based on configuration force method for *r*-adaption together with weighted Laplacian smoothing and mesh enrichment through *h*-refinement based on estimated discretization error in energy norm. A further reduction in the potential energy and the relative error norm of the system is found to be achieved with combined r-adaption and mesh enrichment (in the form of *h*-refinement). Numerical study confirms that the proposed combined $r-h$ adaption is more efficient than a purely *h*-adaptive approach and more flexible than a purely *r*-adaptive approach with better convergence characteristics.

Keywords r-Adaption, Material Forces, Spring Analogy, Discretization Error

1. INTRODUCTION

There has been a considerable focus on theoretical and computational aspects of adaptive finite element analysis since the earliest works by [2, 23]. The computed error could be based on a-priori or a-posteriori estimators. The latter has gained more popularity because of its robustness. In order to obtain required accuracy of finite element solution with minimum cost, an optimal mesh has to be designed. Such a mesh has minimum potential energy and minimal degrees of freedom for a specified accuracy. The degrees of freedom are distributed in such a manner that error distribution is uniform, indicating a flexible discretization.

Several mesh adaptive techniques, such as h, p, r and s-versions that are widely reported, are designed to optimize a spatial discretization. There have been reports on use of a combination of these methods for better performance [8]. A number of remeshing strategies have been developed to account for the multiple length scale effects, which are caused due to strong discontinuities in solution and steep gradients due to mathematical singularities. Most of these remeshing strategies include error estimation and mesh-to-mesh transfer. Mesh-to-mesh transfer involves interpolation errors during transfer of fields from old mesh to new mesh. Also, the fields on the new mesh are not guaranteed to satisfy nodal force equilibrium. Further, these methods do not possess precise mesh optimality criterion and may not provide optimal mesh. The error associated with mesh-to-mesh transfer coupled with nodal force non-equilibrium may cause numerical instability of the simulation. This has led to the scope of arriving at efficient mesh adaption techniques.

In the r-version of refinement strategy, henceforth called r-adaption technique, the nodes of the discretized domain are relocated iteratively in order to minimize the discretization error, while preserving the number of unknowns and order of approximation of the field variable. Typically, the mesh density increases near the regions of steeper gradients of the field variable as a result. The adaptation criteria for r-adaption as per [15] may be classified according to the procedure used for node relocation. Procedures based on hierarchical error estimators and based on configurational equilibrium concepts form the two broad classifications of r-adaptive procedures.

The r-adaption procedures based on hierarchical estimators consist in formulating the mesh adaptation problem, by using a higher order interpolation to evaluate local errors [15]. The error estimated from the current solution is transformed into a spatial distribution of the mesh parameters, which are used

Received 24 September 2004; in final form 2 June 2005.
Address correspondence to S. M. Sivakumar, Associate Professor, Department of Applied Mechanics, Indian Institute of Technology, Madras, Chennai 600036, India. E-mail: mssiva@iitm.ac.in

to generate adapted mesh for the problem under investigation [16].

In the r-adaption procedure based on configurational equilibrium, mesh optimality is accomplished by minimizing the potential energy in the static case and stationarity of discrete action sum in the dynamic case [19]. The potential energy of the system is dependent on nodal coordinates in addition to the displacement field [3]. Configurational or material driving forces are defined as the conjugate forces to the nodal motion with respect to the potential energy [5, 12] and these forces vanish when the potential energy is a minimum. Further, the minimization of the potential energy reduces error norm due to the orthogonality of error with respect to solution space for linear problems [20]. There has been considerable work on the use of material forces and their equilibrium in a computational setting such as the finite element method [12, 14]. The material force imbalance is due to presence of nodes (nodes can be argued to be discrete defects as they break the translational symmetry of potential energy with respect to translations in reference coordinates). For a homogeneous body in continuous case, linear momentum balance implies material force balance. However, introducing discretization causes non-zero material forces at the inter-element boundaries. In this work, a formulation of nodal errors that is consistent with material force equilibrium has been derived.

The node relocation procedure forms a vital part of r-adaption. The adaption for heuristic estimators is based on the classical spring analogy approach [15] where the finite element mesh is considered as a network of elastic springs with the stiffness coefficients depending on the estimated error on each edge. The nodes are moved until the spring system is in equilibrium. This essentially results in equidistribution of errors at the nodes. The node relocation procedure for configurational force method is based on minimization of potential energy. In literature simple relaxation-type iterative procedures have been used [14, 21]. An improved procedure by using a standard Polak-Rebiere conjugate gradient algorithm was proposed by Thoutireddy and Ortiz [18]. In this work, a modification is introduced to this algorithm for faster convergence.

Optimality of an adapted mesh is intimately linked to accuracy with the criterion for node relocation defined with respect to a given norm or measure of error. An efficient node relocation method is thus required for use with sufficient poise as a whole or part of an adaptive refinement strategy. In the present context we have node relocation procedures that have two different bases for computing the optimal mesh and hence there is a need to establish the preeminence of one technique over the other.

In the present work, the above-mentioned two r-adaption procedures have been implemented. The evaluation of these two methods in light of the adaptive refinement strategy forms the focus of this paper. The qualitative and quantitative aspects of driving force terms and their respective convergence rates during the iteration process form the first basis for comparison. The quality of adapted mesh in terms of distortion metric together with relative energy norm of error at the end of node relocation obtained from the two methods forms the second basis of comparison.

The evaluation is made based on studies conducted on one-dimensional and two-dimensional problems. From a quantitative aspect, although both are post-processing techniques, it is empirically and numerically shown that driving force from conventional approach is an upper bound to the driving force arising from configurational force method. From a qualitative angle the sound mathematical basis of deriving the material force procedure makes it a reliable indicator, unlike the spring analogy approach, which is heuristic and involves approximation errors. Further, the configurational force method provides a better physical insight into the problem. From a convergence point of view, the standard Polak-Rebiere conjugate gradient algorithm has been found to be efficient. The proposed two-step linear projection technique improves conventional iterative procedure. For a given discretization, the spring analogy approach has slow convergence. Mesh adaption by configurational force method results in a more flexible more discretization because of increased potential energy than the spring analogy approach.

In the spring analogy approach, at lower node relocation iterations the amount of element distortion and energy norm of discretization error is less. The method poses limitations at higher node relocation iterations in terms of highly distorted meshes and increased energy norm of discretization error. Furthermore, even for lower node relocation iterations the method requires proper choice of correction factors.

The comparative study presented here thus emphasizes the use of an r adaption procedure based on material forces. The suitability of this method has been studied for structured and unstructured meshes together with a weighted Laplacian smoothing. The study shows that a combined $r - h$ strategy resolves the unhealthy mesh distortions and provides better convergence of the solution.

The paper is arranged as follows: The following section describes the two procedures — spring analogy approach and configurational force approach with appropriate algorithms for node relocation. This includes the modifications in derivations and algorithms proposed in the present study. A general assessment of the two techniques is done in a subsequent section. The equivalence of the two techniques for one-dimensional problems and comparison of the two methods in terms of computed driving force and convergence rates studied are also reported in this section. The last section deals with the discussion of the results obtained in implementation of the above methods for one- and two-dimensional problems leading to a scope for combined $r-h$ refinement strategy.

2. DESCRIPTION OF r-ADAPTION TECHNIQUES

The essence of performing the r-adaption is to predict the characteristics of the optimal mesh where the number of degrees

of freedom is distributed in such a manner that accuracy of solution obtained is the highest possible [15, 17]. The errors due to discretization or approximation occurring at the nodes are typically equally distributed for better solution over the entire domain. Two recent methods of r-adaption are analyzed and compared. One is a direct approach, which seeks to equally distribute the error metric based on energy norm associated with the Hessian of the displacement field, while the other seeks to achieve material force equilibrium. Henceforth, the first one will be termed as spring analogy method and the other as configurational force method.

2.1. Spring Analogy Approach

The adaption procedure based on the classical spring analogy approach considers the finite element mesh as a network of elastic springs with stiffness coefficients depending on estimated error on each edge. The error is assumed to be proportional to the Hessian of the interpolation function. Various procedures for computation of the Hessian based on recovery of derivatives are presented. Using this assumption, an adaption criterion that achieves an equidistribution of error along the edges of the elements is adopted. Considering the equilibrium of springs at each node, the driving force and direction of node movement is evaluated (see Figure 1). The discretization error over each element arising due to approximation is given by $e(x) = u(x) - u_h(x)$, where $u(x)$ is the exact solution and $u_h(x)$ is the piecewise continuous approximation of the displacement. The estimator here is said to be hierarchical in the sense that the error $e(x)$ can be estimated as the difference between a smoothed or recovered higher order approximation $\hat{u}_h(x)$ and finite element approximation $u_h(x)$.

Consider a domain denoted by Ω (Figure 2 (a)) and bounded by Γ_D and Γ_N such that $\Gamma_D \cap \Gamma_N = 0$ and $\Gamma_D \cup \Gamma_N = \Gamma$. Let a partial differential equation be defined in Ω as $-\nabla^T(a\nabla u) + f + bu = 0$. Where $\nabla$is the Laplacian operator and u is the unknown function; b and f may be constants or functions depending upon the nature of problem to be modeled. The geometric or Dirichlet boundary conditions take the form $u = \bar{u} = 0$ on Γ_D and natural or Von Neumann boundary conditions are defined as $a\frac{\partial u}{\partial n} = q$ on Γ_N. Considering a specific case of the above equation with $a(x) = EA$ and $b(x) = 0$, the governing equation takes the form $-\frac{d}{dx}(\frac{du}{dx}) = \frac{q(x)}{AE}$, with boundary conditions $u(x = 0) = 0$ and $\frac{du}{dx}(x = l) = 0$. Physically, this equation represents a bar fixed at one end ($x = 0$) and stretched by a body force $q(x)$.

Consider a discretized model consisting of the standard two degrees of freedom bar element. Let us assume that area A, elastic moduli E are constant and that the load is integrated consistently. It is seen that (Figure (2b)) the solution at the nodes is exact and hence the error at the nodes is zero (although the exact solution in general is not piecewise linear and there is error between the nodes). A quadratic approximation of the error over the element can thus be constructed on each element once the value of the second derivative is known. The variation of error

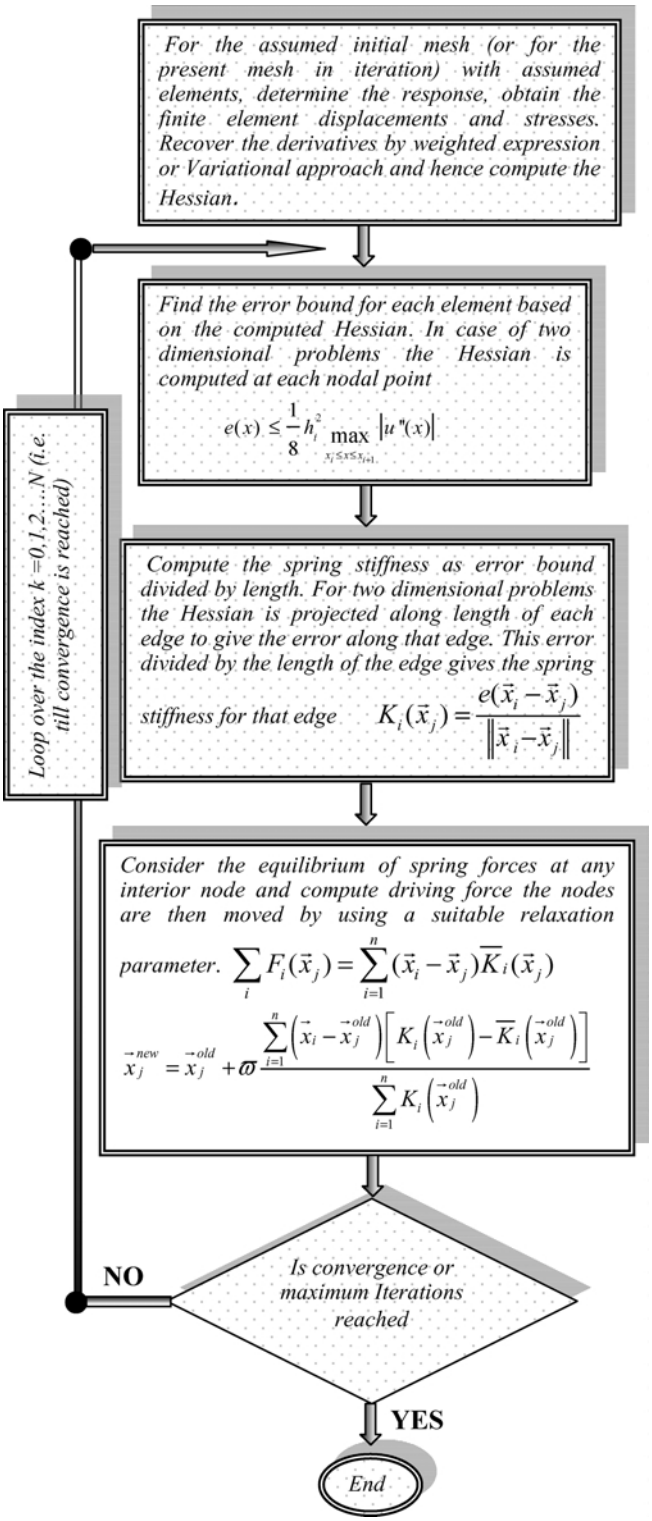

FIG. 1. Steps in node displacement procedure — spring analogy.

over the element length h can be expressed as

$$e(z) = -\frac{1}{2}(x_i - z)^2 e''(z) \tag{1}$$

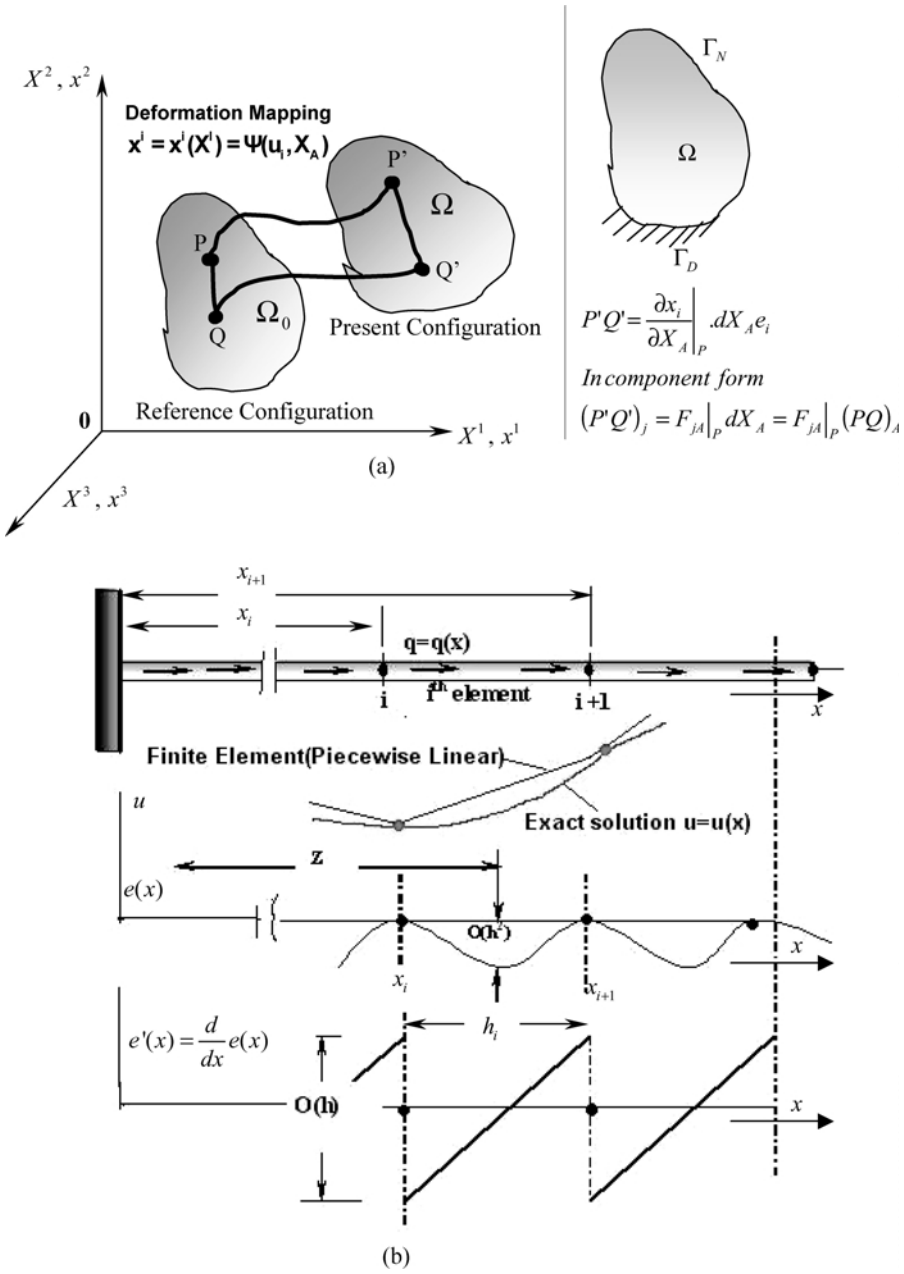

FIG. 2. (a) Solid in reference and deformed configuration. (b) Behavior of error in a uniform bar under distributed axial load.

Where z is any point within the element closer to nodal coordinate x_i than x_{i+1}, i.e. $|z - x_i| \leq h_i/2$. It is seen from the above equation that the error norms are proportional to the second derivatives (Hessian H) of $u(x)$ and must be determined with special care to obtain meaningful results.

Thus we have

$$\|e\| \alpha h_i^2 \frac{\partial^2 u}{\partial x^2}\Big|_{|z-x_i| \in [0,h_i]} \tag{2}$$

We can obtain an upper bound to the maximum error (pointwise) in a given element as

$$|e(\bar{x})| \leq \left(\frac{h_i^2}{8}\right)[\max_{x_i \leq x \leq x_{i+1}} |u''(x)|] \tag{3}$$

The first derivative of the computed solution is piecewise constant and discontinuous across element boundaries. Therefore straightforward differentiation of $u_h(x)$ leads to a second derivative, which is zero inside each element and is not defined at element boundaries. The methodology for computing Hessian is made as per convenience. In the analytical derivation given

TABLE 1
Method of recovery of the second derivatives

Weighted expression	Variational method
$\left.\frac{\partial^2 \vec{u}_h}{\partial x_i \partial x_j}\right\|_k = \frac{\int_{\Omega_k} \frac{\partial \eta}{\partial x_i}\frac{\partial \vec{u}_h}{\partial x_j} d\Omega_k}{\int_{\Omega_k} \eta d\Omega_k} = \frac{\int_{\Omega_k} \frac{\partial N_k}{\partial x_i}\frac{\partial \vec{u}_h}{\partial x_j} d\Omega_k}{\int_{\Omega_k} N_k d\Omega_k}$	$\left.\frac{\partial \vec{u}}{\partial x_i}\right\|_k = \langle P(x_{1k}, x_{2k})\rangle [A]^{-1} \sum_{i=1}^{m} \{P(x1, x2)\} \left.\frac{\partial \vec{u}_h}{\partial x_i}\right\|_{c_g}$
Ω_k is bounded domain $= \sum_{e=1}^{ne} \Omega_e$	$[A] = \sum_{e=1}^{nc} \{P(x_{1e}, x_{2e})\}\langle P(x_{1e}, x_{2e})\rangle$
ne = number of elements connected to interior node k	i and $j = 1, 2$, $\langle P(x_1, x_2)\rangle = \langle 1\ x\rangle$
N_k = Test function—Basis of η_k	$\frac{\partial \vec{u}_h}{\partial x_i}$ = derivative of finite element displacement
Ω_e = Domain of element-element volume	Computed at barycenter of element
	P = Polynomial fit of desired order for the patch considered
	A = Matrix of unknown coefficients

in Appendix I the Hessian matrix at any node k is obtained by following a weighted expression of second derivatives and in numerical computation the Hessian is evaluated by computing the local value of the gradient by ensuring a least square fit of this to the set of super convergent sampling points existing in the bounded domain (Table 1).

In two dimensions the adaption criterion is looked upon as requirement of a mesh that achieves an equidistribution of appropriate error $e(x)$ along the finite element edges E. If τ_E is the unit tangent to edge E, the second derivative along the τ_E-direction is given by $\frac{\partial^2 u}{\partial \tau_E^2} = \tau_E^T H \tau_E$. The error along any edge E is given by

$$e_{kl} = \left(h_{kl}^T H h_{kl}\right)^{\frac{1}{2}} \tag{4}$$

where $h_{kl} = x_k - x_l$ is the length of the edge E with vertices x_k and x_l. When the Hessian matrix is not semi-positive definite the spectral decomposition of Hessian is considered [15].

2.1.1. Node Relocation Procedure

For the mesh movement algorithm, the element sides are considered as springs of prescribed stiffness and the nodes are moved until the spring system is in equilibrium. The stiffness constants proportional to the edge based errors are given by

$$K_i(\vec{x}_j) = \frac{e(\vec{x}_i - \vec{x}_j)}{\|\vec{x}_i - \vec{x}_j\|} \tag{5}$$

where $\vec{x}_i$ are the coordinates of the node i among the n nodes connected to the node j with coordinate $\vec{x}_j$. The ideal position of the node $\vec{x}_j$ is computed from a non linear energy minimization problem and is given by

$$\sum_i F_i(\vec{x}_j) = \sum_{i=1}^{n} (\vec{x}_i - \vec{x}_j)\bar{K}_i(\vec{x}_j),$$

where

$$\bar{K}_i(\vec{x}_j) = \frac{1}{n} \frac{\sum_{i=1}^{n} e(\vec{x}_i - \vec{x}_j)}{\|\vec{x}_i - \vec{x}_j\|} \tag{6}$$

The nonlinear problem defined by the above equation is solved using an iterative procedure algorithm as shown in Figure 1, which starts from an initial guess $\vec{x}_j^{old}$ and $\vec{x}_j^{new}$ is given by

$$\vec{x}_j^{new} = \vec{x}_j^{old} + \varpi \frac{\sum_{i=1}^{n} \left(\vec{x}_i - \vec{x}_j^{old}\right)\left[K_i\left(\vec{x}_j^{old}\right) - \bar{K}_i\left(\vec{x}_j^{old}\right)\right]}{\sum_{i=1}^{n} K_i\left(\vec{x}_j^{old}\right)} \tag{7}$$

where ϖ is a relaxation parameter that controls the convergence.

2.2. Configurational Force Method

The adaption procedure based on configurational forces considers the imbalance in material equilibrium as a measure of error. The departure from material equilibrium is reduced by minimization of the potential with respect to nodal coordinates. This is accomplished by relocating nodes in a finite element mesh. Considering material force equilibrium results in defining energy momentum tensor in material space [3]. The components of the energy momentum tensor represent the change of total potential energy of a deformed body produced by unit material translation. For a homogeneous body, in the continuous case, force balance implies material force balance. However, in the discrete case nodal force balance does not imply nodal material force balance due to the presence of nodes and hence element interface. Thus in a discretized form considering the material force equilibrium, the non-vanishing of the divergence of energy momentum tensor at the inter element boundaries is taken as an error indicator [10].

In this section the error indicator is derived by considering the material force equilibrium in a similar manner as is done in physical equilibrium. The displacement vector for a solid in the region $\Omega_0 \in \Re^3$ (see Figure 2a) in referential description is given as $u_i = x_i - X_i$. The deformation mapping for a lagrangian description is defined as

$$x_i = x_i(X_1, X_2, X_3, t) \Rightarrow x_i = x_i(X_I) \text{or} \Rightarrow \Psi(u_i, X_A) \tag{8}$$

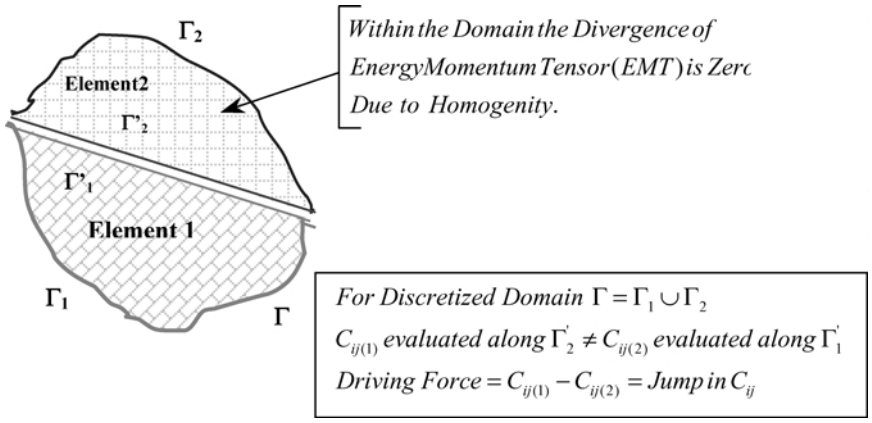

FIG. 3. Jump in driving force at interelement boundaries.

With the deformation gradient in Ω_0 given by $F_{iA} = \delta_{iA} + u_{i,A}$. The deformation mapping takes on prescribed values $\bar{\Psi}$ over the displacement part of $\Gamma(\Gamma = \Gamma_D \cup \Gamma_N)$ of the undeformed boundary. The strain energy density per unit volume of the undeformed elastic material is given by

$$W = W\left(x^i_j, X^K\right) \text{ or } W = W(u_{i,j}, X^K) \tag{9}$$

for an isotropic material $W = \frac{1}{2}\sigma_{ij}\varepsilon_{ij}$, where σ_{ij} is the stress tensor and ε_{ij} is the strain tensor. The physical equilibrium equation is given by $\sigma_{ij,j} + f_i = 0$, where f_i is the body force. The material gradient of strain energy results in the configurational force equilibrium and is given by

$$C_{kj,j} + g_k = 0 \tag{10}$$

where the configurational stress tensor is given by $C_{kj} = W\delta_{kj} - \sigma_{ij}u_{i,k}$ and the configurational force arising due to body forces are given by $g_k = -f_i u_{i,k}$. It is required to compute the discrete configurational forces arising out of discretization. In the absence of body forces the weighted residual form of the balance law equation using a vectorial test function η and integrating over the domain Ω_0 is given by

$$\int_{\Omega_0} C_{ij,j}\eta_i d\Omega_0 = 0 \tag{11}$$

The weak form of this equation (Eq. (11)) in the absence of body forces is obtained by integrating by parts and can be written as

$$-\int_{\Omega_0} C_{ij}\eta_{i,j}d\Omega_0 + \int_{\Gamma} C_{ij}n_j\eta_i d\Gamma + \int_{\Gamma_e \not\subset \Gamma} C_{ij}n_j\eta_i d\Gamma = 0 \tag{12}$$

As a consequence of considering stationary boundaries, the test function η vanishes on the boundaries of the domain Γ and hence the second term becomes zero. The divergence of the energy momentum tensor is zero for a homogeneous body without body forces. This is used to check the discrete solution obtained through finite element analysis. As finite element solutions are approximate solutions, the non-vanishing divergence of the energy momentum tensor provides an error indicator. The discrete jump in the energy momentum tensor (Figure 3) occurring at the element boundaries Γ_e (third term of the weak form equation) is the driving force used as an error measure in the node relocation process. The balance law in its weak form is analogous to the bilinear form of the governing differential equation with jump in the energy momentum tensor being similar to the traction jump occurring at the inter element boundaries [11]. The discretized form of the above weak form can be written by inserting an element–wise interpolation of the test function η and its gradient. Thus we can write

$$\eta_i = \sum_I N^I \eta^I_i \quad \text{and} \quad \eta_{i,j} = \sum_I N^I_{,j}\eta^I_i \tag{13}$$

Thus Eq. (12) reduces to the form

$$\sum_I \left[-\int_{\Omega e} C_{ij}N^I_{,j}d\Omega_0 + \int_{\Gamma_e \not\subset \Gamma} C_{ij}n_j N^I_i d\Gamma \right]\eta^I_i = 0 \tag{14}$$

The second term, which is a traction related to the discontinuity, is the configuration force of the element that needs to be numerically evaluated. Since η_I are arbitrary, each of the above in the summation over I should go to zero. Thus, the first term is equal to the negative of the second that is evaluated as the discrete configuration force, G^I_e, given by

$$\int_{\Gamma_e \not\subset \Gamma} C_{ij}n_j N^I_i d\Gamma = \int_{\Omega e} C_{ij}N^I_{,j}d\Omega_0 = \begin{Bmatrix} G^I_{e1} \\ G^I_{e2} \end{Bmatrix} = G^I_e \tag{15}$$

These configurational forces on assemblage should go to zero in the domain. This also means that the configurational forces of the elements are equidistributed for an optimal mesh. The assembled total configurational force is given by $G^K = \bigcup_{e=1}^{ne} G^I_e$ where ne spans over the number of elements connected to a particular node.

2.2.1. Node Relocation Procedure

The interior nodes are updated by an iterative rule such as $X^K = X^K - cG^k$ [14]. The constant c is chosen sufficiently

small to achieve convergence (to avoid unhealthy mesh distortions). For better convergence a nonlinear conjugate gradient method, known as the Polak-Rebiere method [19], for minimization of energy function has been incorporated. The basis of this method is that for a given iterate x_k (weight) and proceeding direction d_k (gradient), a line search is performed along d_k to produce $X_{k+1} = x_k + \alpha_k d_k$ by an amount α_k (learning rate) in a recursive manner to satisfy equilibrium. Rather than imposing α_k (by learning rate), we choose α_k to minimize the potential energy at the new position $G(x_k + \alpha_k d_k)$. The conjugate gradient algorithm thus performs line search at iteration for each conjugate direction. Conjugacy of the gradients is through any matrix A such that $d_{k+1}^T A d_k = 0$. It is preferable to use directions, which are conjugate to Hessian of the function G, i.e., $\nabla^2 G = A$. For a general error function it is not possible to determine the Hessian. Hence it is desired to have conjugacy without the Hessian. It is desired to have

$$d_k^T A d_j = 0 \quad \text{for} \quad k \neq j \tag{16}$$

The change in gradient at $k + 1$ iteration is given by

$$\Delta G_k = G_{k+1} - G_k = A \Delta x_k$$

where

$$\Delta x_k = x_{k+1} - x_k = \alpha_k d_k \tag{17}$$

This is satisfied if and only if following expressions are satisfied

$$\alpha_k d_k^T A d_j = 0 \quad \Delta x_k^T A d_j = 0 \quad \Delta G_k^T d_j = 0 \tag{18}$$

The first expression in Eq. (17) requires determination of α_k expressed in terms of the Hessian for a pure quadratic as $\alpha_k = \frac{-G_k^T d_k}{d_k^T A_k d_k}$. For a pure quadratic we can write $A_k = \nabla^2 G(x)|_{x=x_k} = x_k^T A x_k$. The last expression definition doesn't require Hessian determination. Thus we start with the initial gradient and we write $d_0 = -G_0$. By line search minimization we can write $d_k = -G_k + \beta_k d_{k-1}$. We define β_k for Polak-Rebiere algorithm as $\beta_k = (\frac{\Delta G_{k-1}^T G_k}{G_{k-1}^T G_k})$.

The algorithm has been explained in Figure 4. The method has two levels of iteration. The outer loop is the undeformed coordinate iterative update or nodal coordinate update. The nodal coordinate iterative loop contains solution for equilibrium solution for deformed coordinate for a fixed mesh. This ensures that the configurational forces for the undeformed coordinate update correspond to the equilibrium solution.

The conventional iterative method of nodal updating in the configurational force method takes a number of iterations to optimize the mesh and hence there is a need to reduce the number of iterations. It is proposed to use a linear projection method, which is similar to the successive over relaxation iterative technique. Here the configurational forces in each node act as an error and the new nodal position for each node is determined by enforcing this error to be zero. Moving one node point modifies

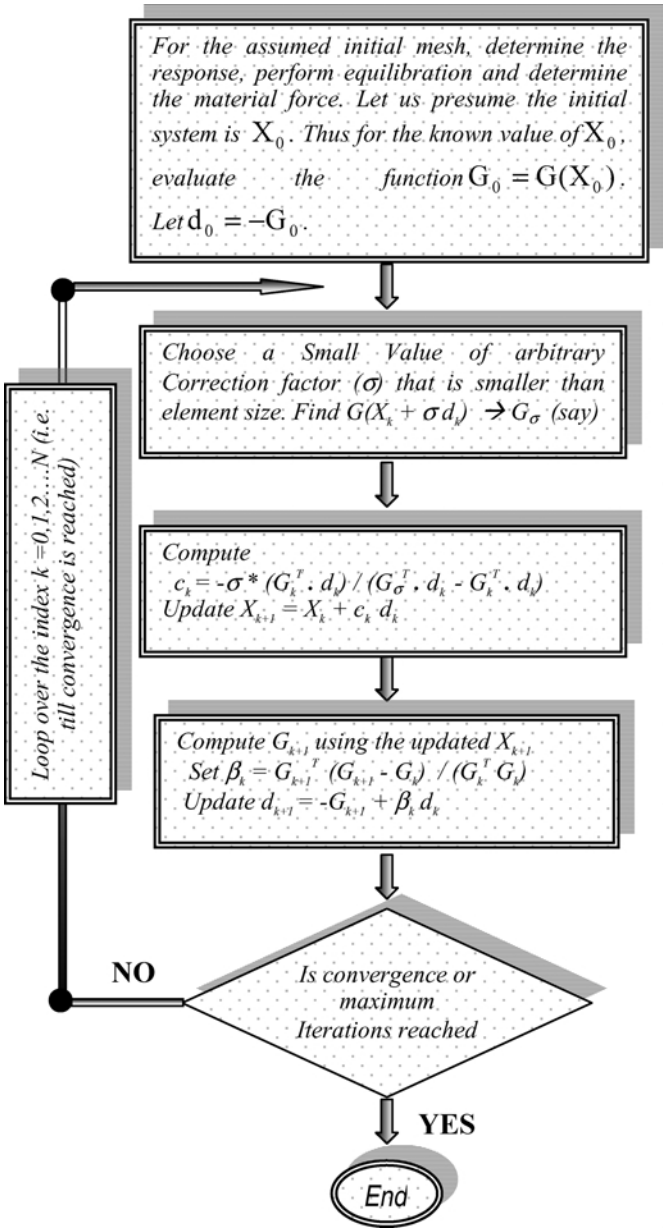

FIG. 4. Steps in node displacement procedure-Polak reberie algorithm.

the surrounding elements, hence the node movement strategy and correction for error is repeated several times throughout the domain. The process being independent for each node, it is seen that the error propagates like a wave, which is typical of successive over relaxation technique. The error wave dies down as the iteration continues. This method takes a few iterations to obtain an optimized mesh.

Let Gx_1, Gx_2, Gx_3 be the driving force terms in the successive iterations 1, 2 and 3, respectively. Let the corresponding node positions at these iterations be x_0, x_1, x_2, respectively. Using similar triangles, knowing two preceding values, the driving force in the third successive iteration is equated to zero and

we can evaluate the node position in this iteration as $x_2 = (\frac{x_0 * Gx_2 - x_1 * Gx_1}{Gx_1 - Gx_2})$.

3. ASSESSMENT OF NODE RELOCATION TECHNIQUES

The need to establish the preeminence of one node relocation technique over the other is important in the context of obtaining better adaptive finite element solutions. This study is expected to help in the use of the better method with sufficient poise as a whole or part of an adaptive refinement strategy. In this section, analytical and numerical comparisons of the configurational force method with the spring analogy method are presented. The assessment is made firstly based on qualitative and quantitative aspects of driving force terms along with their respective convergence rates in potential energy during the node displacement iteration process. Secondly, the quality of the adapted mesh is studied based on the amount of discretization error and the extent of distortion that has occured. The discretization error is computed as the relative percentage error in energy norm. The extent of distortion is measured through a distortion metric.

3.1. Qualitative Analysis

It is presumed and expected that an optimization procedure considering the nodal coordinates as unknowns in the minimization of potential energy results in highly nonlinear equations and with nonlinear constraints of the nodal coordinates, thus making the solution tedious and time-consuming. However, the configurational force method is based on a sound mathematical basis relating to the material force equilibrium, and the non-satisfaction of energy momentum tensor at the inter-element boundaries acts as an error indicator. In a computational setting the resulting nonlinear equations can be iteratively solved using a standard nonlinear solution algorithm.

The interpolation based error estimator associated with the spring analogy approach for node movement is heuristic and thus involves approximation errors. The recovery of the second derivatives, which define the Hessian for a given element and hence its transformation to determine the edge spring stiffness, is quite an involved procedure. The positive definiteness of the Hessian is not assured and depends on the location of the element with respect to the loading and thus further requires spectral decomposition. Further, the node relocation procedure, although based on equilibrium of springs, requires the specification of an error criterion for node movement. The sound mathematical basis of deriving the material force procedure thus makes it a reliable procedure.

The governing differential equation of a problem may be formulated on the basis of the balance laws and constitutive relations. The significance of balance laws and the correspondence of those in physical (physical equilibrium) and material space (material force equilibrium) are evident. Thus defining the energy momentum tensor with its components representing the change of total potential energy of a deformed body produced by unit material translation adds to a better understanding of the problem considered. Thus an adaption procedure considering non-vanishing of the divergence of energy momentum tensor due to inhomogenity as an error indicator gives more physical sense.

3.2. Quantitative Analysis

3.2.1. Driving Force and Convergence

The amount of driving force at a node varies according to the intensity of loading and geometry of the domain, with higher values in the regions of stress concentration. Thus, a quantitative analysis cannot be made for the entire domain but the relative intensities can be compared at a given nodal point as is done in the subsequent section. From a quantitative aspect, although the node relocation made to achieve equilibrium of spring forces at a node in the spring analogy approach is analogous to making the corrections for the driving force arising out of the configurational force equilibrium, the driving force from the conventional approach is an upper bound to those from the configurational force method. This is clear from the derivations for the driving forces in each of these procedures for a one-dimensional case shown in Appendix I.

Convergence of Adaption Procedure: Analysis of the relative convergence is of importance as it reflects the quality of the adaption achieved through node relocation. The correction factor c and relaxation parameter ω respectively govern the number of iterations required for the solution to converge in either method. The quantity of driving force being different in either method, it is preferred to compare the number of iterations required for convergence. The standard Polak-Rebiere iterative algorithm used in the material force method has a faster convergence compared to the conventional iterative technique in terms of number of iterations required to achieve the prescribed tolerance. The convergence rate of the spring analogy approach is less compared to the configurational force method. Further, the relaxation parameter ω in the spring analogy approach has to be carefully chosen to be small enough to avoid unhealthy mesh distortions.

3.2.2. Mesh Quality

A comparative study on mesh quality is important. Mesh quality is assessed in terms of flexibility of discretization by computing the relative amount of change in discretization error and the amount of distortion that is assessed by computing the distortion metric.

The flexibility of the system is assessed through the amount of decrease in potential energy of the system during mesh adaption iterations. The potential energy of the system as obtained from configurational force method asymptotically reduces more than the spring analogy approach and reaches a constant value. Hence a convergence criterion based on potential energy is ideally suited for the configurational force method. In the case of spring analogy approach, although, there is an initial reduction in potential energy at lower iterations at higher iterations, there is a progressive increase in potential energy. The discretization error during the node relocation iterations is computed based on

a best guess stress type error estimator. The error in energy norm is computed as

$$\|e\| = \left(\int_{\Omega} \{e_\sigma\}^T |C|^{-1} \{e_\sigma\} d\Omega \right)^{1/2} \tag{19}$$

where $\{e_\sigma\} = \{\sigma^*\} - \{\sigma_h\}$.

$\{\sigma\}^*$ and $\{\sigma_h\}$ are the best guess stress, and finite element stress, respectively. The best guess stress is obtained through a simple projection technique as given by [24]. The absolute value of the error over domain is calculated. The relative percentage error η is given by

$$\eta = \frac{\|e\|}{\|u\|} * 100 \tag{20}$$

where $\|e\|$ is a suitable error norm and $\|u\|$ is the displacement norm. It is observed that in comparison to spring analogy approach, although the amount of decrease in relative error norm percentage during node relocation iterations is less in case of the configurational force method at initial iterations, there is a progressive rapid increase in error norm percentages at later iterations. The error norm percentage based on post-processed stress does not provide much information on mesh quality. Since the topology of the mesh is retained during node relocation, a better estimate of mesh quality and efficiency of mesh adaption would be in terms of the extent of the element distortion that occurs in the node relocation procedure. The distortion metric is computed based on geometric properties as

$$D = \sum_{i=1}^{n} \sum_{j=1}^{n} M_{ij}^2 - \frac{1}{n} \left(\sum_{k=1}^{n} M_{kk} \right)^2 \tag{21}$$

where $M_{ij} = \frac{1}{\det |J|} \sum_{k=1}^{n} J_{ki} J_{kj}$, n = 2 for two-dimensional problems, J is the Jacobian matrix.

The distortion metric is zero for a square element and increases as a power of four with the aspect ratio or angular distortion. The one- and two-dimensional examples considered for numerical comparison of these methods in the next section give additional insight into the finer issues related to the use of each of these methods.

3.2.3. Type of Mesh

The suitability of the two mesh adaption procedure for the type of initial meshes chosen is important. In general a mapped or structured mesh is more suitable for mesh adaption. Even for a structured mesh the spring analogy approach results in highly distorted meshes leading to degeneracy with the steps of node relocation iterations. The configurational force method performs well for both structured as well as unstructured mesh. At higher node relocation iterations the method requires a smoothing procedure to avoid degeneracy. A weighted Laplacian smoothing approach has thus been implemented to avoid degeneracy. The basic idea of the well-known Laplacian smoothing method is to place a node in the center of its neighboring nodes. The node is to be repositioned by directly averaging the co-ordinates of the neighboring nodes. The movement vector is given by

$$\Delta V_L = \frac{1}{nnode} \sum_{i=1}^{nnode} V_i \tag{22}$$

where $V_i = (x_i - x_0, y_i - y_0)$ and *nnode* is the number of neighbor nodes surrounding the patch node.

3.2.4. Enhancement by Mesh Enrichment

It is observed that there is no change in the topology of the domain when corrections are made for configurational forces. There is only an increase or decrease in the element size h_i. The aim of adaptive post-processing technique is to obtain softer discretization, along with stationary value of potential and to get better displacement or stress solution across element boundaries with a good mesh. The criteria for goodness of mesh are based upon strain energy, displacement and stress values at selected critical points of a structure. Mesh adaption tends to result in bad shape elements and approximation. This is from the understanding that the displacement polynomial approximation made within the element assumes extreme values at the nodes. To get better finite element solution we need to change the topology of the domain once the stationary value of the potential is reached after completion of mesh adaption iterations. Furthermore an optimal mesh is one in which the number of degrees of freedom is minimal for a specified accuracy. This can be achieved only through mesh enrichment. The process of adaption and enrichment may follow one another as one single cycle or may be repeated in cycles.

4. RESULTS AND DISCUSSIONS

In this section we report the results of numerical tests that establish the effectiveness of the method of r-adaption. Numerical comparison of the two methods considered give additional insight into the finer issues related to use of each of these methods and thus helps in establishing the superiority of one node relocation technique over the other and thereby obtaining better adaptive finite element solutions.

4.1. One Dimensional Example

A linear elastic axial rod fixed at the one end, and free at other end, which is under a uniform body force b as shown in Figure 5(a), was considered for the implementation and comparison of the configurational force and the spring analogy method in one dimension. The displacement solution for this axial rod is given by $u(x) = \frac{b}{E}(x - \frac{x^2}{2})$, where E is the Young's modulus of material. Here we chose E = 1 N/m^2 b = 1 N/m. Corresponding to this displacement the strain and stress are linear in x. This suggests that uniform mesh is the optimal mesh corresponding to this solution. To authenticate this by mesh adaption, the elastic rod is discretized using linear elements as shown in Figure 5(b). A set of six nodes were considered

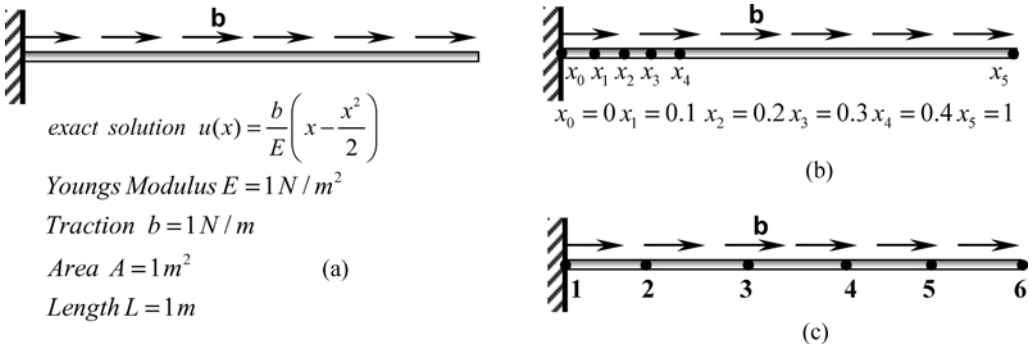

FIG. 5. (a) Cantilever beam subjected to uniform traction. (b) Initial mesh of linear elements. (c) Optimal uniform adapted mesh.

with one node at the free end to define geometry and other nodes clustered near to fixed end. Mesh adaption based on configurational forces and spring analogy approach was performed with appropriate relaxation, correction factors ϖ and C, respectively. Figure 5(c) as expected shows the final adapted optimal uniform mesh. Both the methods result in a uniform mesh.

Quantitative analysis was made for elastic rod subjected to uniform body force. Table 2 shows a comparison of the normalized driving force values obtained at all nodes at the end of first iteration from the two methods. It is observed that the total norm of driving force values considering all nodes in spring analogy method is much higher than that obtained from configurational force method. This is also evident from the derivation for the two element one-dimensional problem shown in Appendix 1. The variation of driving force with iterations in both the methods is different although there is a reduction in the values with iterations. Various parameters, such as the potential energy, stiffness matrix trace and strain energy, are studied during mesh adaption to provide a basis for comparison. It is seen that with iterations the potential energy of the system reduces and reaches a minimum (Figure 6(a)) with the strain energy variation being almost complimentary to potential energy. The driving force is equidistributed between elements at nodes and the net force at a node is zero. The optimality of mesh is also justified from the trace of the stiffness matrix, which reduces and reaches a constant minimum (Figure 6(b)) value, indicating that the adaption procedure results in a flexible system with increased displacement. In the variation of each of these parameters, the spring analogy approach shows a discrete jump in the values after some iteration; this may be attributed to the limitations in recovering the second derivatives at the boundaries.

TABLE 2
Normalized values of driving forces as interior nodes after one node relocation iteration

Interior node number	1	2	3	4
Driving Force	$x_1 = 0.1$	$x_2 = 0.2$	$x_3 = 0.3$	$x_4 = 0.4$
Configurational force	1.0	3.2	2.9	$3.1525e+14$
Spring Analogy	1.0	1.07	$3.695e+14$	$1.2e+14$

For convergence characteristics, different node displacement procedures studied are configurational force method with conventional iterative correction, configurational force method with standard Polak-Rebiere algorithm, configurational force method with linear projection and spring analogy approach. Figure 7(a) gives a comparison of convergence for these methods. From the point of view of number of iterations required to achieve optimality, as expected the Polak-Rebiere algorithm is better than the conventional iterative algorithm. The incorporation of the linear projection method gives accelerated convergence. It is observed that the spring analogy approach has a slow convergence rate compared to the configurational force method. To have an insight of variation of driving force in the spring analogy method, the computed value of the Hessian is plotted at all nodal points along the length of elastic rod as shown in Figure 7(b). It is seen that with mesh adaption the values progressively reduce to a constant along the length.

4.2. Two Dimensional Example

4.2.1. Block Under Pressure

A homogeneous square block of linear elastic isotropic material with nondimensionalized length of four units with a symmetric loading is considered. The vertical displacements on the bottom edge are fixed. The block is discretized using four noded bilinear elements. The initial mesh is shown in Figure 8(a). A plane strain state is assumed. For the given loading and boundary conditions mesh adaption is performed by both the methods using spring analogy and Polak-Rebiere conjugate gradient node relocation algorithms, respectively, to get adapted mesh as shown in Figure 8(b) and Figure 8(c).

A quantitative analysis of the normalized driving force is made as shown in Figure 8(d). In two dimensions it is observed

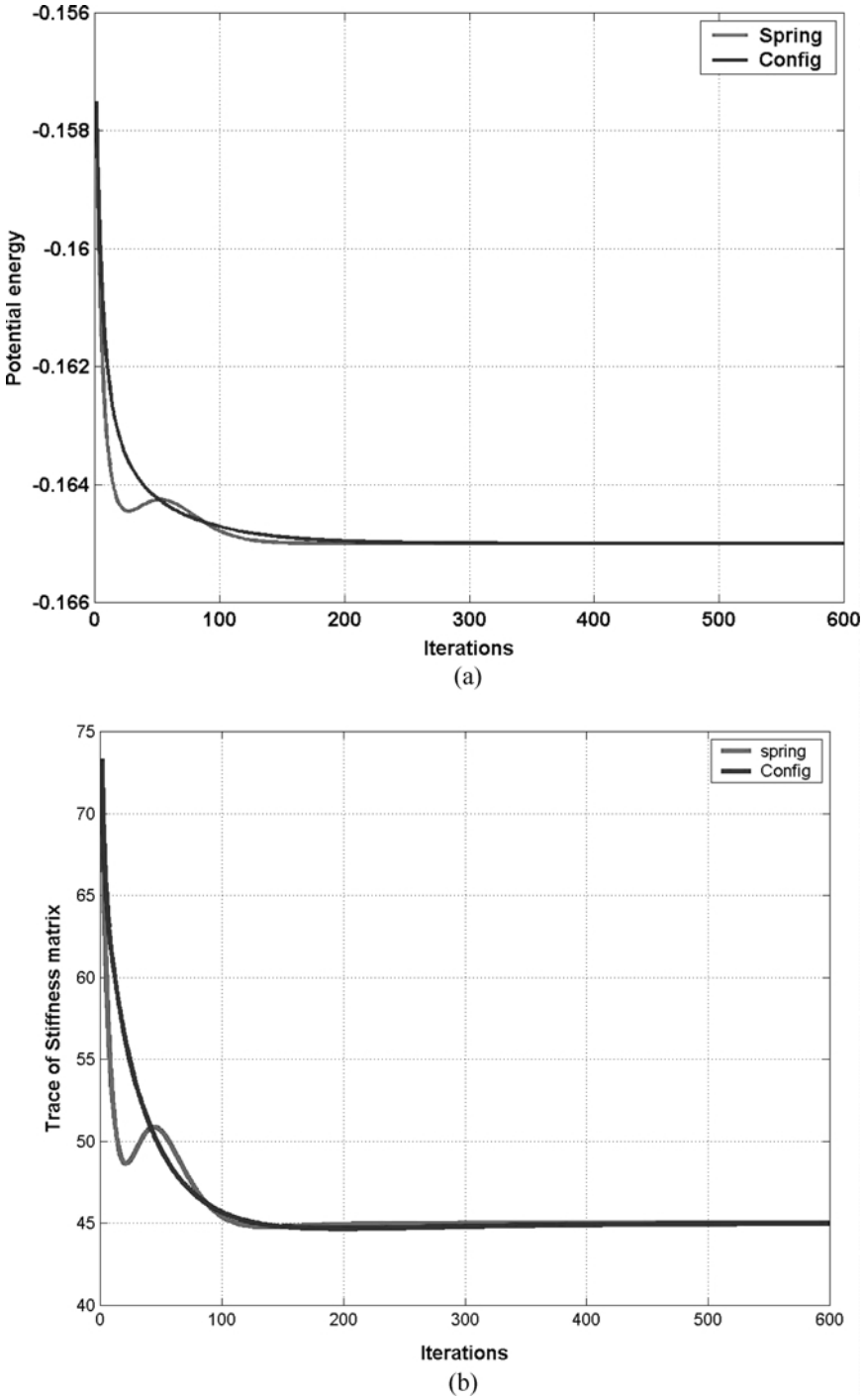

FIG. 6. (a) Comparison of potential energy for various iterations. (b) Comparison of trace of stiffness matrix for various iterations.

that the driving force from the spring analogy is less than the configurational force method. The normalized driving force reduces with iterations in both the methods. The qualitative analysis here is looked at from the point of variation of potential energy of the system with iterations (Figure 9(a)). The spring analogy approach does not result in a flexible system as in the configurational force method, hence the energy of the system is less. This is also evident from the rigid nature of the adapted mesh obtained from the spring analogy approach. Similar to one dimension, the convergence rates are slower and more care is required in choosing appropriate value of relaxation parameter.

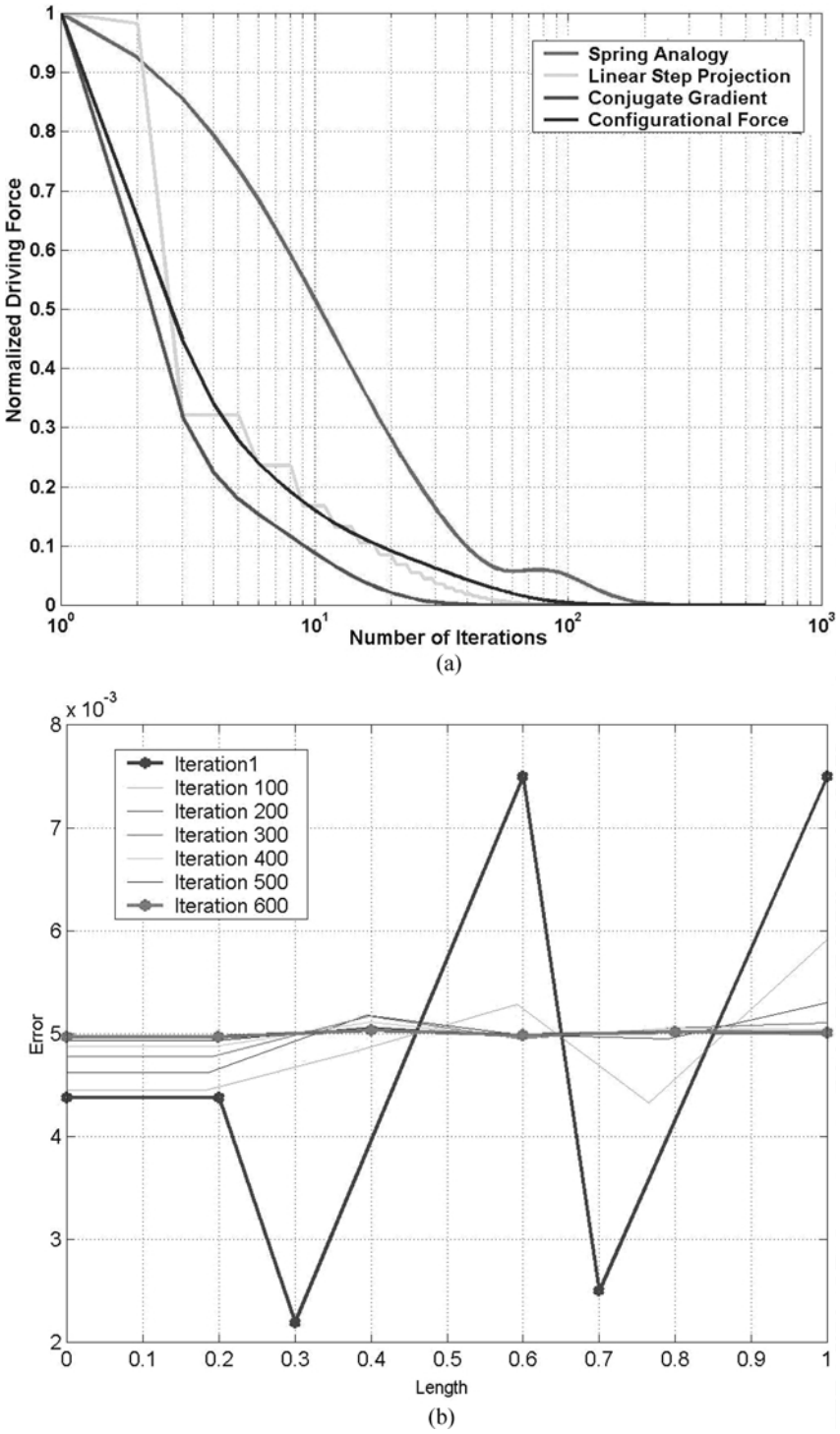

FIG. 7. (a) Comparison of convergence rates for various techniques. (b) Plot of Hessian along the length of elastic rod.

The mesh quality is assessed in terms of extent of reduction in discretization error and distortion of elements. From Figure 9(b) it is seen that the relative percentage of energy norm error is less in the case of the spring analogy approach at initial iterations, but at later iterations owing to large amount of distortion and subsequent degenracy there is a progressive increase in the energy norm error. The distortion metric is computed for each of the individual elements as shown in Figures 10(a) and 10(b). The distortion metric contours for configurational force based adapted mesh indicate a

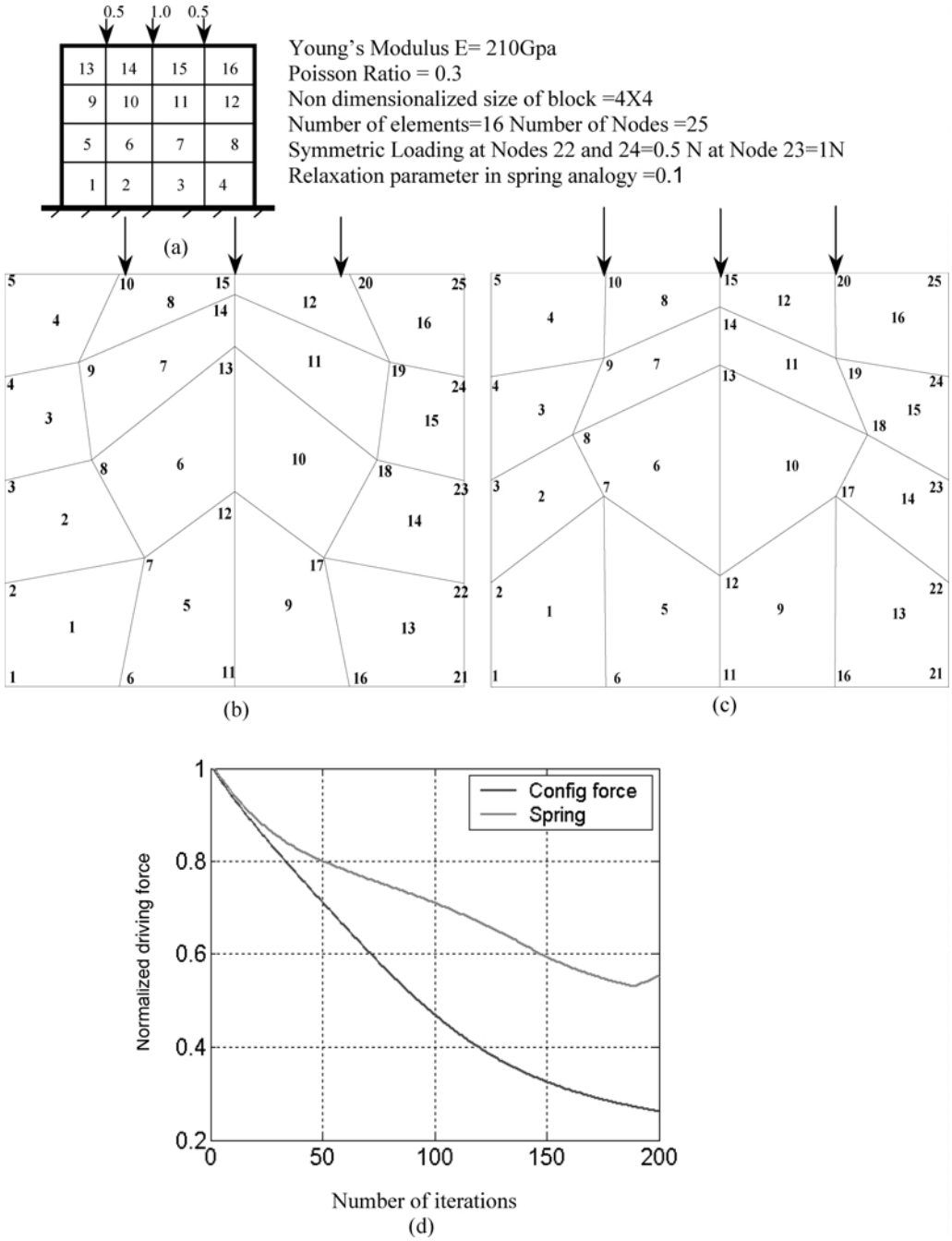

FIG. 8. (a) Block under pressure (initial mesh. (b) Final mesh obtained from configurational force method. (c) Final mesh obtained from spring analogy. (d) Plot of normalized driving force versus number of iterations.

coencetric distortion of elements close to the applied load while in the case of the spring analogy approach it is more distributed.

The mesh adaption has dependency on strain energy. It is thus important to study the distribution by plotting contours of strain energy density function, which are called isoenergetics. These indicate contour shape along which the nodes of an element can be aligned. A plot of constant strain energy density (isoenergetics) for the block is shown in Figure 11(a) and Figure 11(b). It is observed that there is a low strain gradient after adaption due to spreading of contours. As expected, the strain energy density matches with degree of freedom density in the sense that the nodes move towards and align themselves on these contours after adaption. The properties of an optimal adapted mesh can

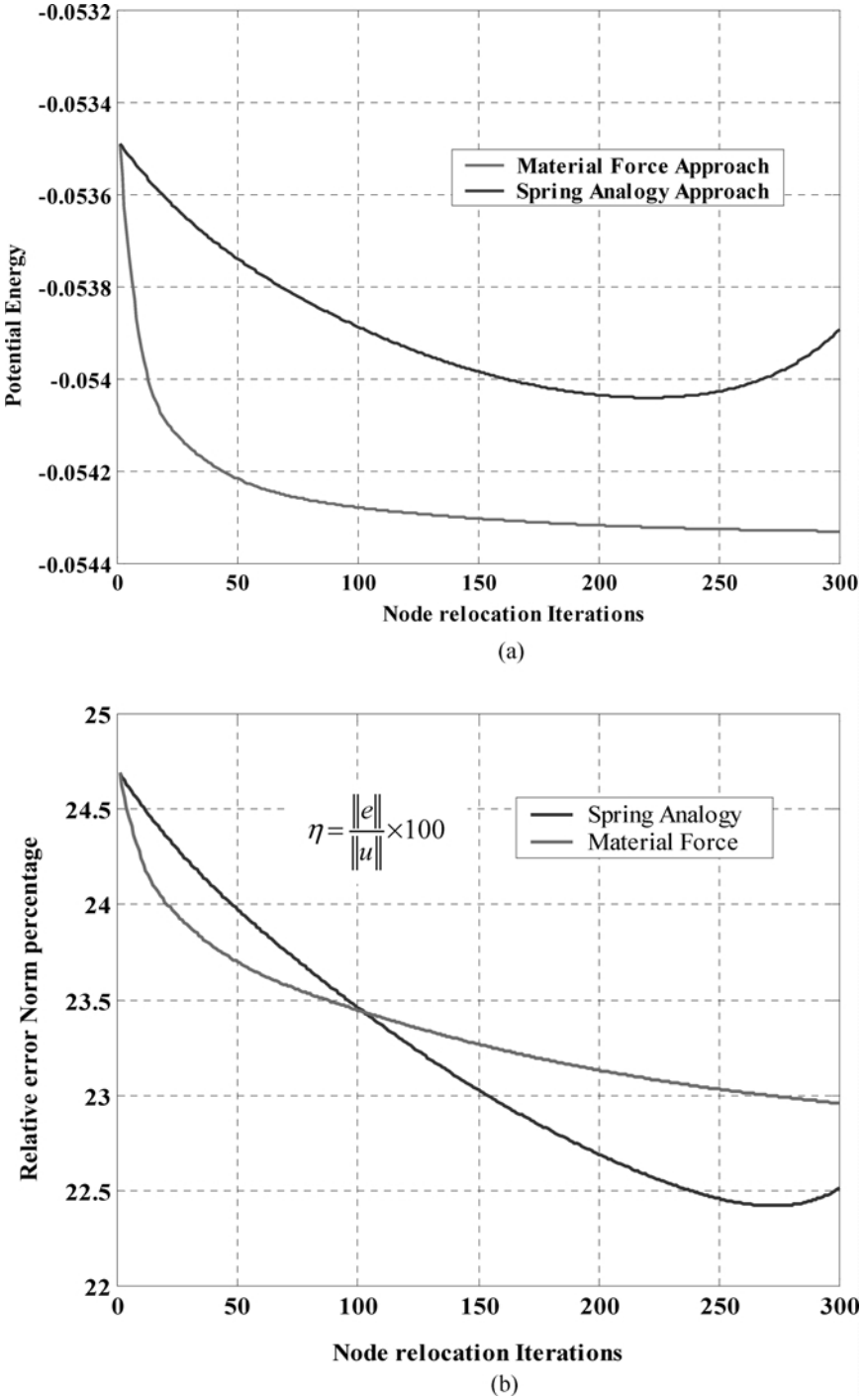

FIG. 9. (a) Comparison of potential energy versus number of iterations. (b) Comparison of relative error norm versus iteration.

also be looked at from several other plots, such as isobars (contours of maximum principal stress) and isochromatics (contours of maximum shear stresses). A plot of the Isochromatics of the block is plotted as shown in Figure 11(c). Resultant mesh after adaption has nodal points coinciding with the isochromatics of the problem.

4.2.2. L-Shaped Domain

A homogeneous L-shaped domain of linear elastic, isotropic material (Young's modulus = 70 Gpa and Poisson ratio = 0.33) is considered with specified dimensions and loading. A plane stress state is assumed. The domain is discretized using four noded bilinear elements. For the given loading and boundary

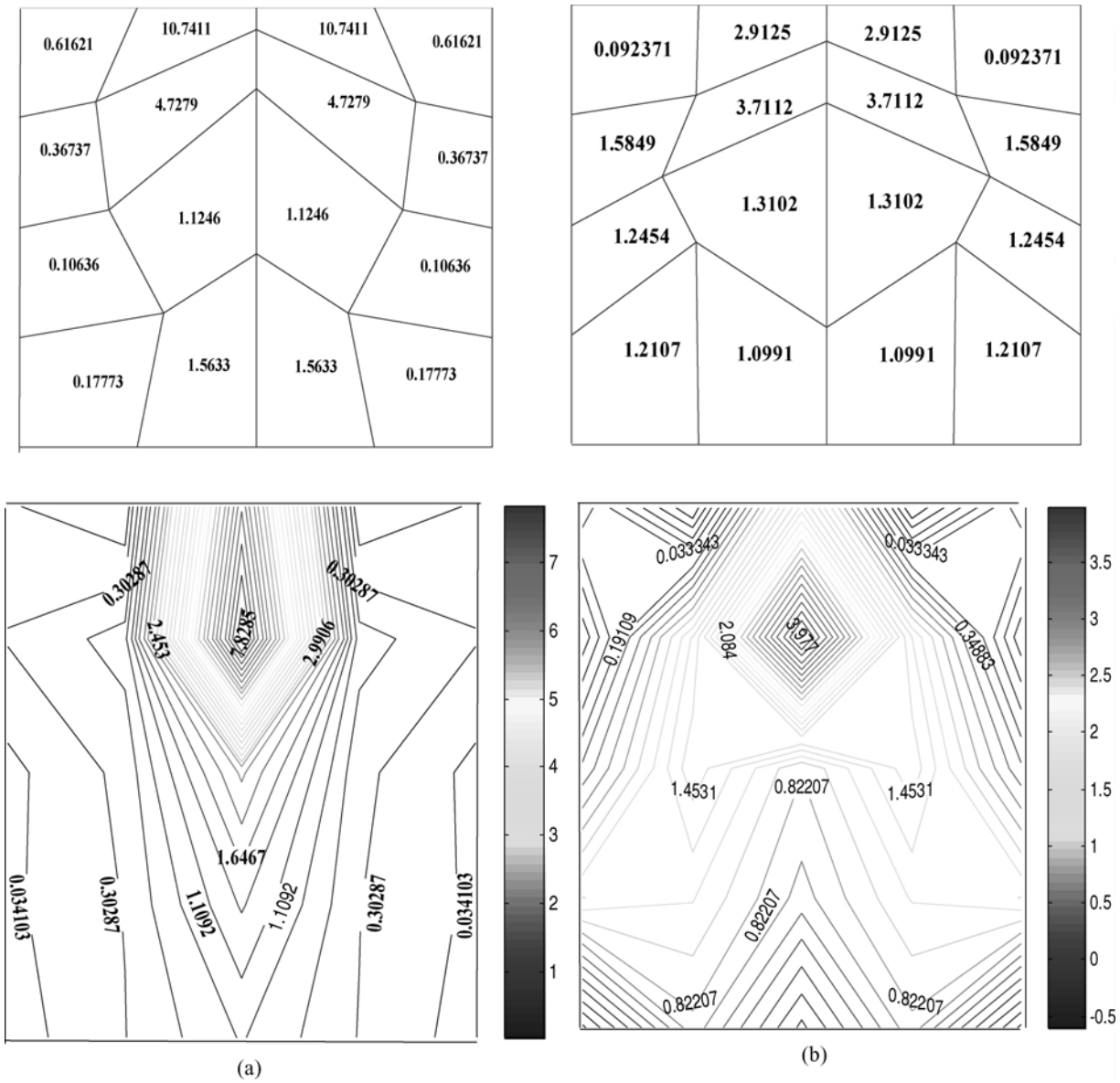

FIG. 10. (a) Distortion metric and contours — material force method. (b) Dsitortion metric and contours — spring analogy approach.

conditions mesh adaption based on configurational force is performed using Polak-Rebiere conjugate gradient algorithm. The suitability of the mesh adaption by configurational force method has been studied for structured and unstructured meshes.

Structured mesh: The initial structured discretization is as shown in Figure 12(a). The adapted mesh after certain number of iterations is shown in Figure 12(b). It is reported in literature and also observed here that the mesh adaption results in distorted and degenerate elements. It is required to continue the adaption procedure for further minimization of potential at the same time it is required to avoid degeneracy. In this context a weighted laplacian smoothing is performed to smooth the elements. This is highlighted in the next section. The variation of the potential energy with iterations with an intermediate smoothing is shown in Figure 13(a).

Unstructured mesh: The initial unstructured mesh is as shown in Figure 14(a). It is seen that the extent of degeneracy of elements with iterations in unstructured case increases (Figure 14(b)). To avoid the degeneracy it is more important to smooth the mesh between the iterations. Figure 14(c) shows the mesh after weighted laplacian smoothing. Figure 14(e) shows the potential energy variation with iterations (with an intermediate smoothing to avoid mesh degeneracy effects). From the earlier examples of elastic rod and block under pressure it is seen that the criterion for convergence decides the number of iterations and reflects the quality of estimated driving force during

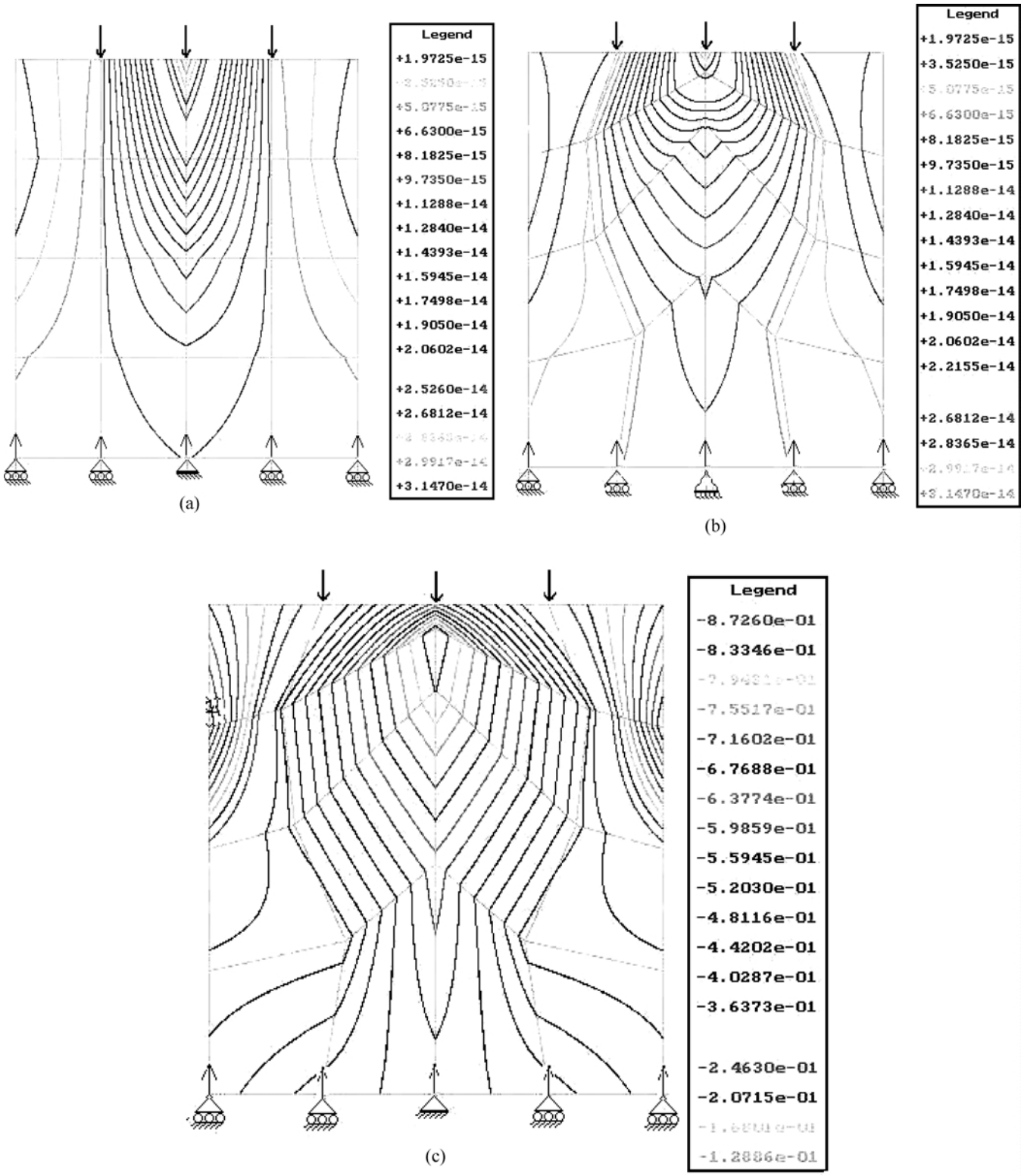

FIG. 11. (a) Isoenergetics—strain energy before adaptation. (b) Isoenergetics—strain energy after adaptation. (c) Isochromatics—contours of maximum shear stress.

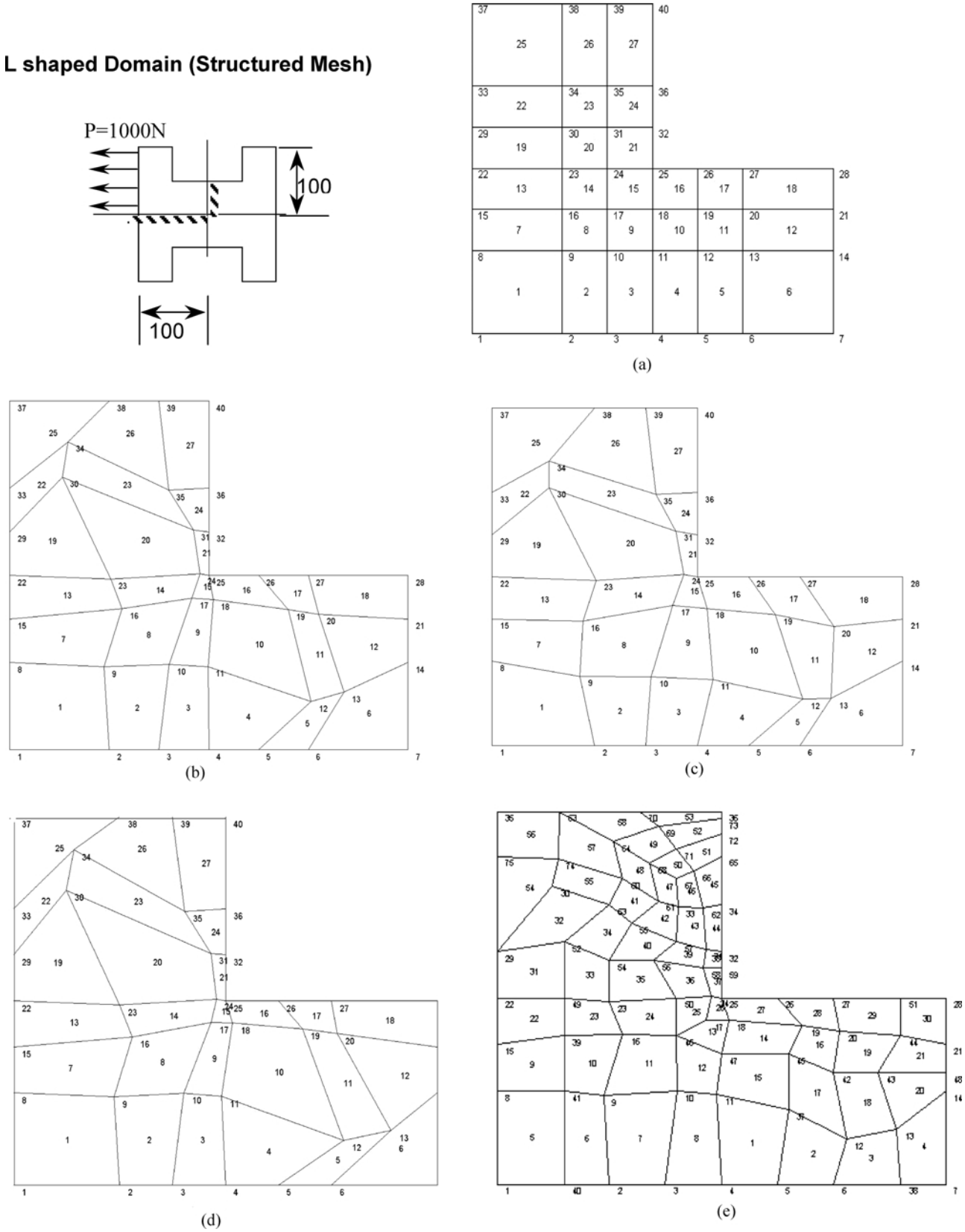

FIG. 12. (a) Initial structured mesh before adaptation. (b) Mesh before smoothing (700 iterations). (c) Mesh after smoothing. (d) Final mesh after all conjugate gradient iterations. (e) Smoothed and enriched mesh.

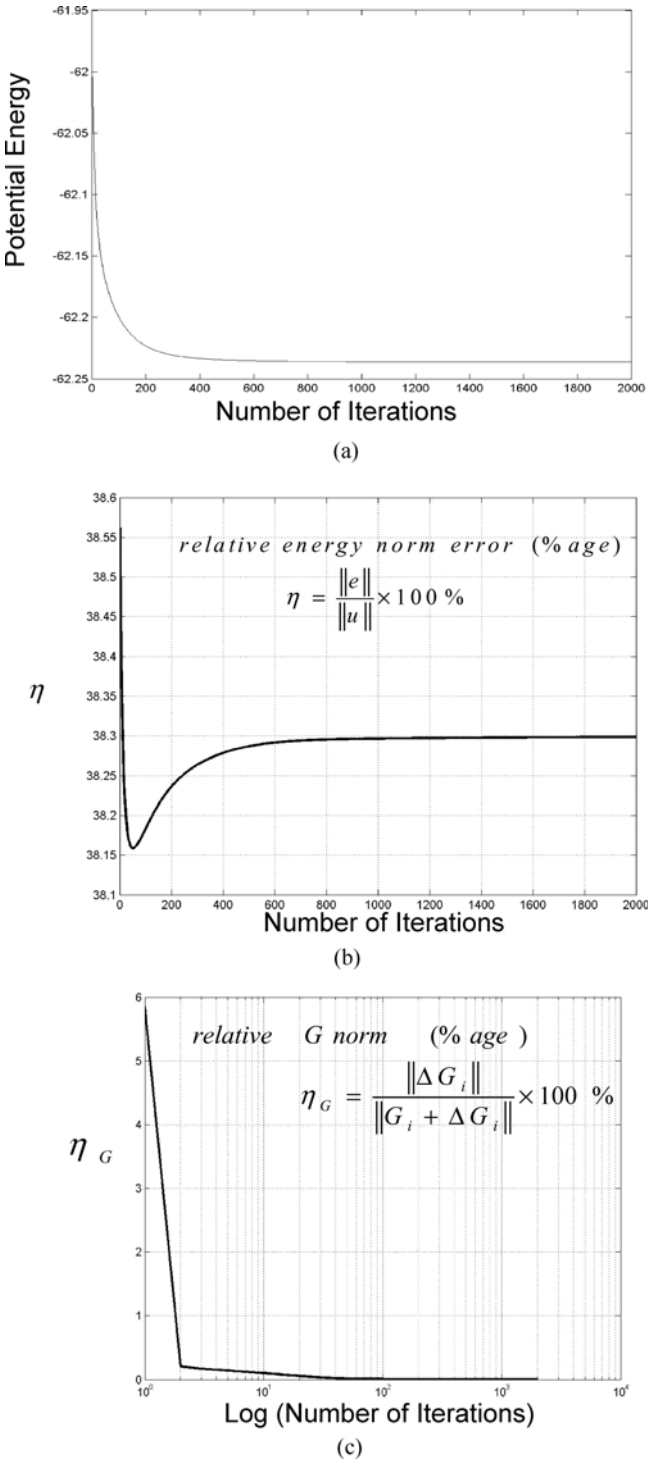

FIG. 13. (a) Potential energy versus number of iterations. (b) Relative error norm percentage versus number of iterations. (c) Relative G norm percentage versus number of iterations.

iteration. A modified criterion is required for the following reasons. A tolerance criterion based on configurational forces or potential energy is stringent and results in large number of iterations. Further smoothing or any such procedure during node relocation is likely to affect the potential energy and the configurational forces. A measure to account for variability in initial meshes for a given problem is thus required. A possible efficient way is to prescribe the relative percentage change in configurational force given by

$$\text{relative } G \text{ norm } (\%\text{age}) \ \eta_G = \frac{\|\Delta G_i\|}{\|G_i + \Delta G_i\|} \times 100\% \quad (23)$$

$\|G_i\|$ is the cumulative elemental value of the configurational force at the end of every iteration. Similarly we can find the global value by adding up all the elemental values and can be denoted as $\|G_i\|_g$. The variation of η_G educes with iterations, indicating that the system reaches a stationary value of the potential. If $\bar{\eta}_G =$ spicified value of η_G, we get a measure of tolerance in considering the stationary value of the potential. We can thus define $\bar{\eta}_G =$ spicified value of η_G for specifying the shift in equilibrium from the viewpoint of configurational force mesh adaption. The variation of relative error norm percentage and global G norm percentage over the mesh adaption iterations for the structured mesh are shown in Figure 13(b) and Figure 13(c) respectively. Figure 14(e) and Figure 14(f) shows the variation of potential and relative error norm percentage with iterations for the unstructured mesh. The relative error norm percentage decreases initially with adaption owing to the increase in the flexibility of the system. With adaption there is progressive distortion of the element and with topology being preserved, the approximations of the field variable and hence the recovery based error estimator tends to be bad. This is reflected through the increase in the value of the error norm percentage at later iterations. The effect of smoothing mesh is reflected in the plots of potential and relative error norm percentage (Figure 14(e) and Figure 14(f)). The smoothing tends to reduce the error norm percentage and potential. It is thus expected that η would increase with the iterations made for node relocation. This is likely in many elements of the initial mesh. It is also likely that in some elements the relative error norm percentage reduces.

It is seen that on the whole the extent of distortion is almost same in either methods. A closer look indicates that the spring analogy approach results in stiffer discretization with elements having less distortion metric values while the configurational force method results in flexible discretization with elements having higher distortion metric values. Further, since the intention is to use the suitable adaption technique as a part of a combined refinement strategy, which may incorporate mesh enrichment through h-refinement, the efficiency of method on the basis of distortion metric for elements is less important. The reduction in error norm percentage is observed when r adaption is followed by mesh enrichment by h-refinement in succession, the final adapted and enriched meshes for a specified value of global error norm for both the examples are shown in Figure 15(a) and Figure 15(b). The plots of convergence characteristics of combined r-h strategy indicates the efficiency of the method.

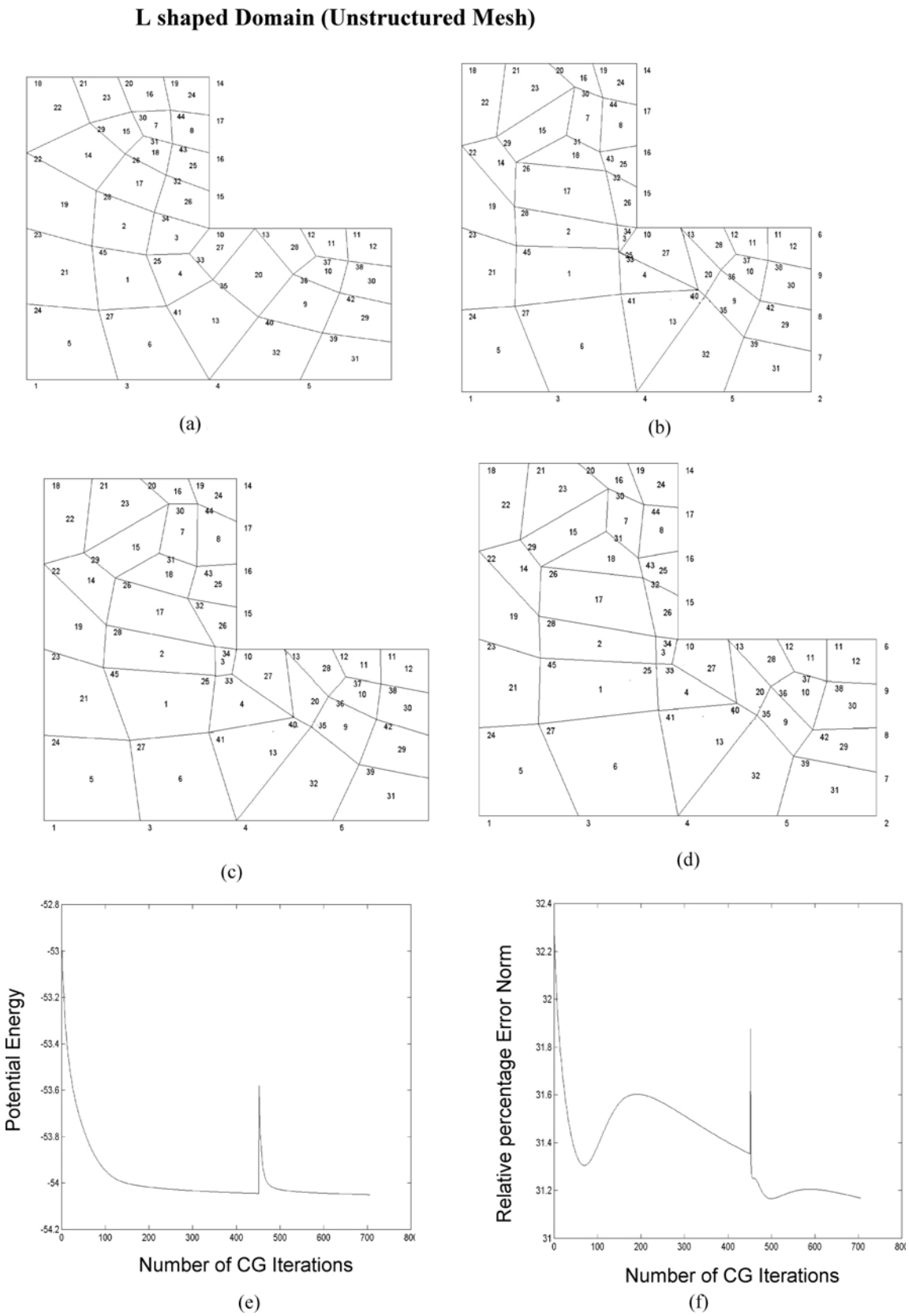

FIG. 14. (a) Initial unstructured mesh. (b) Mesh after 500 CG Iterations (before smoothing). (c) Mesh after 500 CG Iterations (after smoothing). (d) Final mesh after adaptation. (e) Potential energy vs number of iterations. (f) Relative error norm vs number of iterations.

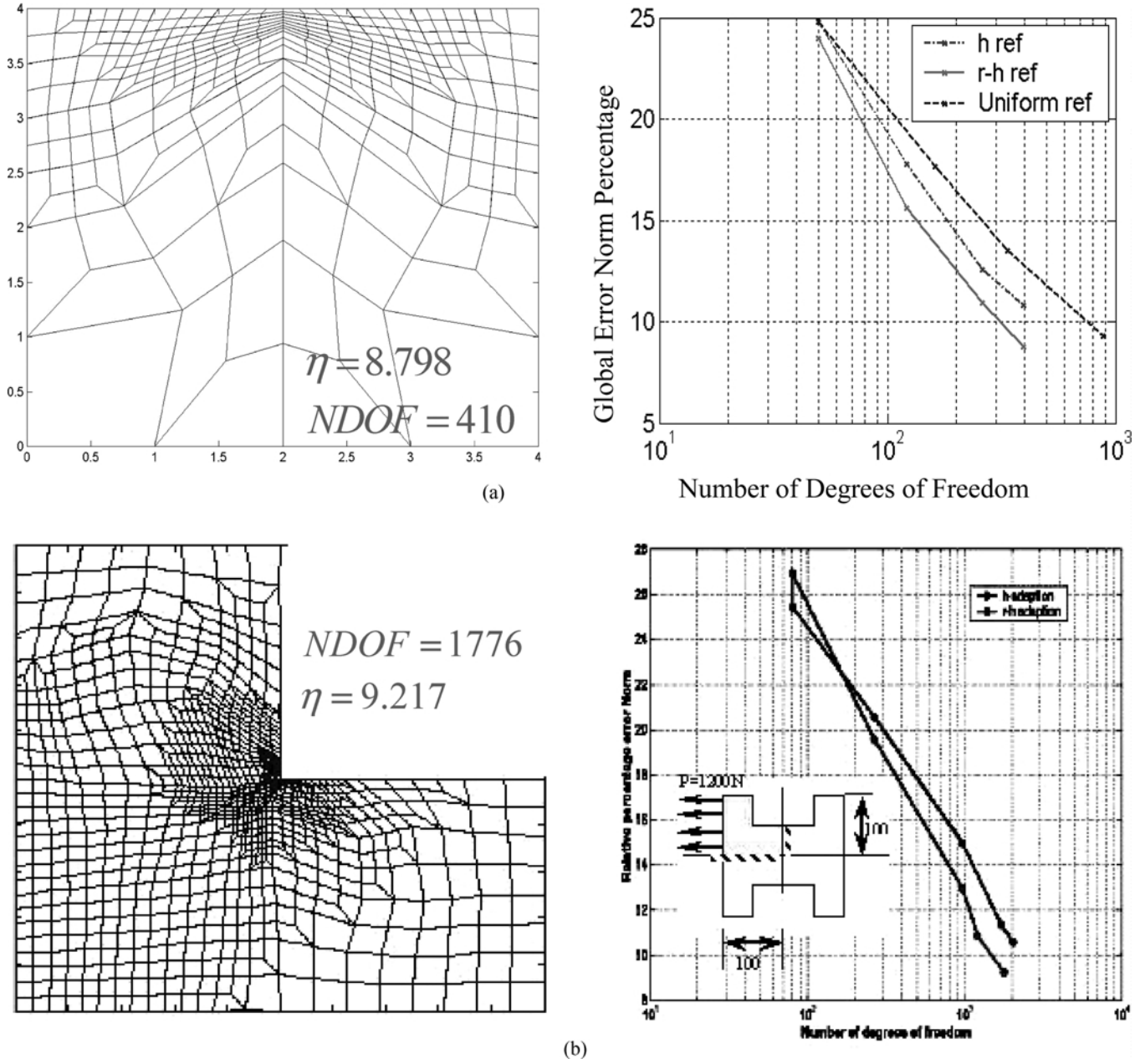

FIG. 15. (a) Final enriched mesh and error norm convergence for example of block under pressure. (b) Final enriched mesh and error norm convergence for example of L-shaped domain.

5. CONCLUSIONS

Assessment of two r-adaption procedures prevalent in the literature has been made. The evaluation is made based on studies conducted on one-dimensional and two-dimensional problems. The qualitative and quantitative aspects of driving force terms together with their respective convergence rates during the iteration process form the basis for comparison.

From a quantitative aspect, although both are post-processing techniques, it is empirically and numerically shown that the driving force from conventional approach is an upper bound to the driving force arising from configurational energy. From a qualitative angle the sound mathematical basis of deriving the material force procedure makes it a reliable indicator, unlike the spring analogy approach, which is heuristic and involves approximation errors. Further, the configurational force method provides a more physical insight into the problem. From a convergence point of view, the standard Polak-Rebiere conjugate gradient algorithm has been found to be efficient. The proposed

two-step linear projection accelerator improves convergence of the conventional iterative procedure. The spring analogy approach has slow convergence.

Although both procedures may result in unhealthy mesh distortions, in the spring analogy approach the resulting optimal mesh does not minimize the potential energy to the extent that can be obtained from the configurational force approach. The extent of distortion and discretization error is more in the spring analogy at later iterations. In addition, the spring analogy approach requires proper choice of correction factors for good convergence to the optimal mesh. This problem gets magnified, especially in the case of unstructured meshes. The present work thus emphasizes the use of an r adaption based on configurational forces. The suitability of this method has been studied for structured and unstructured meshes along with a weighted Laplacian smoothing procedure to avoid degeneracy. The study shows that a combined r-h strategy resolves the unhealthy mesh distortions and is expected to provide a better convergence of the solution. It is concluded in this study that a combined $r - h$ refinement with configuration force method for r-refinement together with weighted Laplacian smoothing can provide best finite element solutions for problems that involve high gradients of stress, such as in fracture mechanics and other singularity prone problems.

REFERENCES

1. Ainsworth, M., and Oden, J. T., *A Posteriori Error Estimation in Finite Element Analysis.* Wiley Interscience, New York (2000).
2. Babuska, I., and Rheinbold, W. C., "A-posteriori error estimators for the finite element method," *Int. J. Numerical Methods in Engineering* **12**, 1597–1615 (1978).
3. Braun, M., "Configurational forces induced by finite element discretization," *Proc. Estonian Acad. Sci. Phys. Math.* **46**, (1/2), 24–31 (1997).
4. Cook, R. D., Malkus, S. D., and Plesha, M. E., *Concpts and Applications of Finite Element Analysis.* Third edition, John Wiley & Sons, New York (1988).
5. Eshelby, J. D., "The elastic energy-momentum tensor," *Journal of Elasticity* **5**(3–4), 321–335 (1975).
6. Gurtin, M. E., and PodioGuidugli, P., "On configurational inertial forces at a phase interface," *Journal of Elasticity* **44**, 255–269 (1996).
7. Jhon, O'Dow., *A Unified Approach to the Finite Element Method and Error Analysis Procedures*, Academic Press, New York (1998).
8. Jung, Ho-Cheng, "Adaptive grid optimization for structural analysis—geometry based approach," *Computer Methids in Applied Mechanics and Engineering* **107**, 1–22 (1993).
9. Kelly, D. W., "The self-equilibration of residuals and complimentary a posteriori error estimates in finite element method," *Intl Journal for Numerical Methods in Engineering* **20**, 1491–1506 (1984).
10. Kienzler, R., and Herrmann, G., *Mechanics in Material space with Applications to Defect and Fracture Mechanics*. Springer-Verlag, NY (2000).
11. Krishnamoorthy, C. S., and Mukherjee, S., "Adaptive finite element analysis with quadrilateral elements using a new h-refinement strategy," *SADHANA* **21**(5), 623–652 (1996).
12. Maugin, G. A., "Material forces. Concepts and applications," *Applied Mechanics Review* **48**(5), 213–245 (1995).
13. Muller, R., and Maugin, G. A., "On material forces and finite element discretization," *Computational Mechanics* **29**, 52–60 (2002).
14. Muller, R., Kolling, S., and Gross, D., "On configurational forces in the context of the finite element method," *Intl Journal for Numerical Methods in Engineering* **53**, 1557–1574 (2002).
15. Pierre, B., Koko, J., and Touzani, R., "Mesh r-adaption for unilateral contact problems," *International Journal of Applied Mathematics and Computer Science* **12**, 9–16 (2002).
16. Peraire, J., Perio, J., and Morgan, K. "Adaptive remeshing for three-dimensional compressible flow computation," *Journal of Computational Physics* **103**, 269–285 (1992).
17. Scott McRae, D. R., "Refinement grid adaptation algorithms and issues," *Computational Methods in Applied Mechanics and Engineering* **189**, 1161–1182 (2000).
18. Thoutireddy, P., and Ortiz, M., "Variational mesh and shape optimization," *Fifth World Congress on Computational Mechanics, July 7–12*, Vienna. (2002).
19. Thoutireddy, P., *Variational Arbitrary Lagrangian-Eulerian Method. PhD thesis*. Pasadena, CA (2002).
20. Thoutireddy, P., Molinari, J. F., Repetto, E. A., and Ortiz, M. A., "Variational r-adaption and shape-optimization for finite-deformation elasticity," *International Journal for Numerical Methods in Engineering* **60**(12), 1337–1351 (2004).
21. Thompson, J. F., Soni, B. K., and Weatherill, N. P., *Handbook of Grid Generation.* CRC Press, Boca Raton, FL (1999).
22. Yazdani, A. A., Gakwaya, A., and Dhatt, G., "A posteriori error estimator based on the second derivative of the displacement field for two-dimensional elastic problems," *Computers and Structures* **62**, 317–338 (1997).
23. Zienkiewicz, O. C., and Zhu, J. Z., "A simple error estimator and adaptive procedure for practical engineering analysis," *Intl Journal for Numerical Methods in Engineering* **24**, 337–357 (1987).
24. Zienkiewicz, O. C., and Zhu, J. Z., "Super convergence recovery techniques and a-posteriori error estimators," *Intl Journal for Numerical Methods in Engineering* **30**, 1321–1339 (1990).

APPENDIX 1

Comparison of Driving Force in One Dimension

Material force based r adaption Polak-Rebiere algorithm for node relocation	Heuristic estimators based r-adaption Spring analogy approach for node relocation
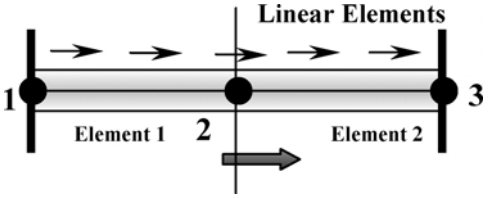	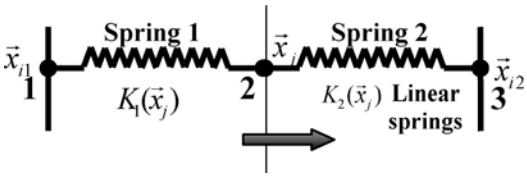
Net force $= \hat{F} = Driving\ force = F_2 - F_1$	Spring stiffness $K_i(\vec{x}_j) = \frac{e(\vec{x}_i - \vec{x}_j)}{\|\vec{x}_i - \vec{x}_j\|}$

(Continued on next page)

APPENDIX 1
Comparison of Driving Force in One Dimension *(Continued)*

Material force based r adaption Polak-Rebiere algorithm for node relocation	Heuristic estimators based r-adaption Spring analogy approach for node relocation
Weak form of the material force equilibrium $-\int_{\Omega_0} C_{ij}\eta_{i,j}d\Omega_0 + \int_\Gamma C_{ij}n_j\eta_i d\Gamma + \int\limits_{\Gamma_e\not\subset\Gamma} C_{ij}n_j\eta_i d\Gamma = 0$ Test function approximation $\eta_i = \sum_I N^I\eta_i^I$ and $\eta_{i,j} = \sum_I N^I_{,j}\eta_i^I N = [\frac{1-x}{l_i}\ \frac{x}{l_i}]$ $\sum_I [-\int_{\Omega e} C_{ij}N^I_{,j}d\Omega_0 + \int_{\Gamma_e\not\subset\Gamma} C_{ij}n_j N_i^I d\Gamma]\eta_i^I = 0$ $\sum_I -\int_{\Omega e} C_{ij}N^I_{,j}d\Omega_0 = \sum_I \int_{\Gamma_e\not\subset\Gamma} C_{ij}n_j N_i^I d\Gamma G^K = \bigcup_{e=1}^{ne} G_e^I$ $C_{ij} = EMT = \psi\delta_{kj} - \sigma_{ij}u_{i,k} = \frac{1}{2}\sigma\varepsilon - \sigma\varepsilon = -\frac{E}{2}\left(\frac{\partial u}{\partial x}\right)^2$ $u = u_{FE} = \sum_I N_i u_i u,\ x = \sum_I N_{,i}u_i N_i = [\frac{1-x}{l_i}\ \frac{x}{l_i}]$ Thus the material force at each of the nodes is given by $-\frac{AE}{2}\left[\frac{1}{l_1}^2(u_2-u_1)^2\begin{bmatrix}1 & 2\\ -1 & 1\end{bmatrix}^T + \frac{1}{l_2^2}(u_3-u_2)^2\begin{bmatrix}2 & 3\\ -1 & 1\end{bmatrix}^T\right]$ Assuming the end nodes to be fixed, the driving force at the interior node when the spans $l_1 = l_2 = l$ are equal are $\frac{-AE}{2l^2}\left[\left(u_1^2 - u_3^2\right) + \left(2u_3u_2 - 2u_1u_2\right)\right]$	Net Force $= \sum_i F_i(\vec{x}_j) = \sum_{i=1}^n (\vec{x}_i - \vec{x}_j)\bar{K}_i(\vec{x}_j)$ $e_l(x) = a_{kl}^T H a_{kl}\ a_{kl} = x_k - x_l =$ length of element where $\bar{K}_i(\vec{x}_j) = \frac{1}{n}\frac{\sum_{i=1}^n e(\vec{x}_i - \vec{x}_j)}{\|\vec{x}_i - \vec{x}_j\|}$ Hessian H is computed using projection technique $H_{ij}(x_k) = \frac{\partial^2\vec{u}_h}{\partial x_i\partial x_j}\big\|_k = \frac{-\int_{\Omega_k}\frac{\partial\eta}{\partial x_i}\frac{\partial\vec{u}_h}{\partial x_j}d\Omega_k}{\int_{\Omega_k}\eta d\Omega_k} = \frac{\int_{\Omega_k}\frac{\partial N_k}{\partial x_i}\frac{\partial\vec{u}_h}{\partial x_j}d\Omega_k}{\int_{\Omega_k}N_k d\Omega_k}\|$ Test function and displacement approximation $u = u_{FE} = \sum_I N_i u_i u,\ x = \sum_I N_{,i}u_i N_i = \left[\frac{1-x}{l_i}\ \frac{x}{l_i}\right]$ $\eta_i = \sum_i N^I\eta_i^I$ *and* $\eta_{i,j} = \sum_i N^I_{,j}\eta_i^I N = \left[\frac{1-x}{l_i}\ \frac{x}{l_i}\right]$ The Hessian after assembly is given by $= -AE\left[\frac{1}{l_1}(u_2-u_1)\begin{bmatrix}1 & 2\\ -1 & 1\end{bmatrix}^T + \frac{1}{l_2}(u_3-u_2)\begin{bmatrix}2 & 3\\ -1 & 1\end{bmatrix}^T\right]$ $\bar{K}_1(\vec{x}_j) = -\frac{AE}{2}\left(\frac{(u_2-u_1)}{l_1^2}\right)/\|l_1\|$ $\bar{K}_2(\vec{x}_j) = -\frac{AE}{2}\left(\frac{(u_3-u_2)}{l_2^2}\right)/\|l_2\|$ Considering equilibrium of springs the driving force at the interior node when the spans $l_1 = l_2 = l$ we get $\frac{-AE}{2l^2}[(u_2-u_1) + u_3 - u_2]$

APPENDIX 2
Nomenclature

$e(x)$, $\|e(x)\|$, e_{kl}	Error function, norm of error function and error along an edge kl
$u(x)$	Exact solution for displacement
$u_h(x)$	Finite element solution
N	Interpolation function used for finite element approximation
$\hat{u}_h(x)$	Smoothed or recovered finite element solution
h_i	Element size
h_{kl}	Length of the edge kl
x_k, x_l	Coordinates of the vertices points of edge kl
H	Hessian matrix
τ_E	Unit tangent to edge E
$K_i(\overrightarrow{x}_j)$	Spring stiffness of an edge
ϖ, c	Relaxation and correction factors
f, q	Body force and traction terms
Ω, Ω_i	Domain and elemental volumes
$\Gamma = \Gamma_D \cup \Gamma_N$	Domain boundary union of Drichlet and Von Neumann boundaries
$\Psi(u_i, X_A)$	Deformation mapping function
X_A, x_a	Referential and present coordinates
F_{iA}	Deformation gradient
$W(u_{i,j}, x_k)$	Strain energy density
σ_{ij}, C_{ij}	Cauchy stress tensor and energy momentum tensor
g_k	Configurational body forces
G_e^I, G^k	Elemental and assembled nodal configurational force
G_{x1}, G_{x2}	Configurational force at successive present configurations
$\|\Delta G_i\|$	Norm of change in configurational force
η_G, η	Relative G norm and Relative error norm (percentages)
$\bar{R}$	Domain residual term representing internal energy
$\bar{F}$	Boundary residual term
$\bar{B}$	Interface boundary residual
$J(a\frac{\partial u_h}{\partial n})$	Jump in the traction values at the element interfaces